

Dissipatively driven entanglement of two macroscopic atomic ensembles

Christine A. Muschik¹, Eugene S. Polzik², and J. Ignacio Cirac¹

¹*Max-Planck-Institut für Quantenoptik, Hans-Kopfermann-Strasse, D-85748 Garching, Germany*

²*Niels Bohr Institute, Danish Quantum Optics Center QUANTOP, Copenhagen University, Blegdamsvej 17, 2100 Copenhagen Denmark.*

Up to date, the life time of experimentally demonstrated entangled states has been limited, due to their fragility under decoherence and dissipation. Therefore, they are created under strict isolation conditions. In contrast, new approaches harness the coupling of the system to the environment, which drives the system into the desired state. Following these ideas, we present a robust method for generating steady state entanglement between two distant atomic ensembles. The proposed scheme relies on the interaction of the two atomic systems with the common vacuum modes of the electromagnetic field which act as an engineered environment. We develop the theoretical framework for two level systems including dipole-dipole interactions and complement these results by considering the implementation in multi-level ground states.

PACS numbers: 03.67.Mn, 32.80.Qk

I. INTRODUCTION

Entanglement is the most prominent and distinctive feature of quantum mechanics. As it plays a central role in fundamental tests of Quantum Mechanics and in applications in the field of quantum information science, entanglement has been generated and studied in various systems. However, experimental generation of entangled states and their use in quantum information and communication protocols is hampered by their fragility under decoherence. The life time of entangled quantum states is typically very short. The pursuit of the generation of persistent entanglement is not only of fundamental interest in view of the investigation of entangled quantum states at long time-scales but also vital for many applications, such as quantum repeaters [1–11]. On account of this problem, quantum systems are usually strictly isolated in the endeavor to avoid their interaction with the environment.

In contrast, we adopt an ostensibly counter-intuitive approach using dissipation [12–46]. Here, the interaction of the system with the environment is employed such that dissipation drives the system into the desired state. More specifically, we propose and analyze a scheme for the generation of long-lived entanglement between two distant, mesoscopic ensembles (see also [47]). Both atomic samples are placed in magnetic fields and interact with an environment consisting of the vacuum modes of the electromagnetic field. A laser field mediates the coupling of the atomic system to the environment. The interaction of the system and the bath can be controlled via laser- and magnetic fields, which allow one to engineer the coupling in such a way that the unique steady state of the dissipative evolution is an entangled state.

This dissipative approach has several remarkable advantages. For example, the scheme performs well starting from an arbitrary initial state. This feature renders the initialization of the system in a pure state unnecessary. Most importantly, the evolution is robust against moderate external noise. Entanglement is obtained in a

steady state. This auspicious property is very promising in view of the quest for viable, extremely long-lived entanglement.

We develop a scheme for two-level systems and show that steady-state entanglement can be generated in the presence of undesired transitions and fluctuating magnetic fields. We also include external pump fields and find that surprisingly, incoherent pumping can be beneficial in a certain parameter range. These central results are supplemented by a short and very general study of the implementation in atoms with multi-level ground states. Since additional dynamics in atoms with multi-level structure lead to particle losses, a quasi-steady state is produced. Remarkably, incoherent pumping enables the creation of entanglement in a true steady state. We investigate the conditions for the generation of long-lived entanglement in mesoscopic multi-level systems, using a simplified model and consider the realization of the proposed method in ¹³³Cs vapors as used in [48–50] as specific example.

The paper is organized as follows. The main idea is introduced in Sec. II, which also contains a summary of the central results. In Sec. III we derive the full master equation for two-level atoms and calculate the evolution of entanglement. Prospects for generating steady-state entanglement in multi-level systems are discussed in Sec. IV. Sec. V summarizes and concludes the paper.

II. MAIN IDEA AND CENTRAL RESULTS

In the following, we explain the basic idea for generating purely dissipatively driven entanglement in atomic ensembles. We introduce a realistic description including noise effects and discuss the prospects for realizing the proposed scheme experimentally.

We start by explaining the underlying concept for two bosonic modes with annihilation operators a and b . The entangled target state under consideration is a two mode squeezed (TMS) state $|\Psi_{\text{TMS}}\rangle$, which is characterized in

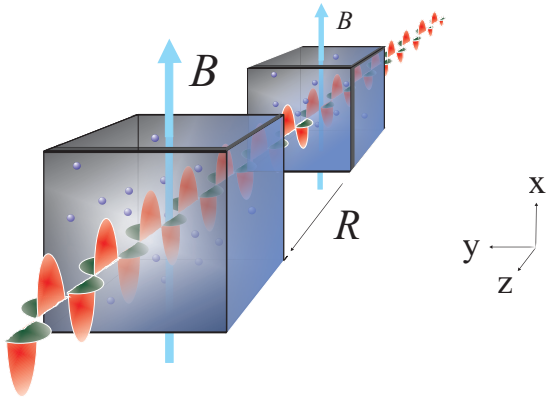


FIG. 1: (Color online) Setup for creating steady-state entanglement between two atomic ensembles separated by a distance \mathbf{R} . Both ensembles are placed in magnetic fields \mathbf{B} , which are oriented along $\hat{\mathbf{x}}$. A strong $\hat{\mathbf{y}}$ -polarization laser beam (shown in green color) propagates along $\hat{\mathbf{z}}$ and couples the atomic system to the environment which consists of the vacuum modes of the copropagating electromagnetic field in $\hat{\mathbf{x}}$ polarization (depicted in red). The interaction between atoms and light modes is illustrated in Fig. 2.

terms of

$$\tilde{A}|\Psi_{\text{TMS}}\rangle = \tilde{B}|\Psi_{\text{TMS}}\rangle = 0,$$

where the nonlocal annihilation operators \tilde{A} and \tilde{B} [51] are given by

$$\begin{aligned}\tilde{A} &= \mu a + \nu b^\dagger, \\ \tilde{B} &= \mu b + \nu a^\dagger.\end{aligned}\quad (1)$$

This equation completely characterizes a particular squeezed state with squeezing parameter r where $\mu = \cosh(r)$ and $\nu = \sinh(r)$. This state can be prepared by means of a dissipative evolution governed by the master equation

$$\begin{aligned}d_t \rho(t) &= \kappa_{\tilde{A}} \left(\tilde{A} \rho(t) \tilde{A}^\dagger - \tilde{A}^\dagger \tilde{A} \rho(t) / 2 - \rho(t) \tilde{A}^\dagger \tilde{A} / 2 \right) \\ &+ \kappa_{\tilde{B}} \left(\tilde{B} \rho(t) \tilde{B}^\dagger - \tilde{B}^\dagger \tilde{B} \rho(t) / 2 - \rho(t) \tilde{B}^\dagger \tilde{B} / 2 \right),\end{aligned}\quad (2)$$

where the coefficients $\kappa_{\tilde{A}}$ and $\kappa_{\tilde{B}}$ are positive. This time evolution drives the system into the unique steady state $\rho_\infty = |\Psi_{\text{TMS}}\rangle\langle\Psi_{\text{TMS}}|$, for $t \rightarrow \infty$ (see App. A).

Starting from this result, we explain how this concept can be applied for creating entanglement between two macroscopic atomic ensembles and how a dissipative evolution of type (2) can be realized. We consider two atomic ensembles placed in magnetic fields as shown in Fig. 1. Atoms are assumed to possess a two-level ground state with internal states $|\uparrow\rangle$ and $|\downarrow\rangle$ (see Fig. 2). We aim at creating an entangled state, where the collective spins of the two samples are correlated in $\hat{\mathbf{y}}$ and in $\hat{\mathbf{z}}$ direction. The amount of entanglement generated can be measured

by the quantity [49, 52]

$$\xi = \frac{\text{var}(J_{y,I} + J_{y,II}) + \text{var}(J_{z,I} - J_{z,II})}{|\langle J_{x,I} \rangle| + |\langle J_{x,II} \rangle|}. \quad (3)$$

For separable states $\xi \geq 1$. $J_{x,I} = \sum_{i=1}^{N_I} j_{x,I}^i$ is the collective spin in $\hat{\mathbf{x}}$ direction in the first ensemble, where N_I is the number of atoms and $j_{x,I}^i$ is the $\hat{\mathbf{x}}$ -spin component of the i th atom [53]. Analogous definitions hold for spins in $\hat{\mathbf{y}}$ and $\hat{\mathbf{z}}$ direction and for the collective spin of the second ensemble. In order to prepare this target state, we use a dissipative evolution governed by a master equation of type (2), where the nonlocal operators \tilde{A} and \tilde{B} are replaced by

$$\begin{aligned}A &= \mu J_I^- + \nu J_{II}^+, \\ B &= \mu J_{II}^- + \nu J_I^+.\end{aligned}\quad (4)$$

$\mu, \nu \in \mathbb{R}$ and $J_{I/II}^\pm$ are collective spin operators [54], with $J^- = \frac{1}{\sqrt{N}} \sum_{i=1}^N |\uparrow\rangle_i \langle\downarrow|$ and $J^+ = \frac{1}{\sqrt{N}} \sum_{i=1}^N |\downarrow\rangle_i \langle\uparrow|$ such that $J_y = \frac{1}{2}(J^+ + J^-)$ and $J_z = \frac{i}{2}(J^+ - J^-)$. Normalization of the operators $[A, A^\dagger] = [B, B^\dagger] = 1$ requires $\mu^2 - \nu^2 = 1$. The light-matter interaction shown in Fig. 2 gives rise to the desired master equation. More specifically, after adiabatic elimination of excited states, the effective ground state Hamiltonian is of the form $H \propto \int_{\Delta\omega_{ls}} d\mathbf{k} (A a_{\mathbf{k}}^\dagger + A^\dagger a_{\mathbf{k}}) + \int_{\Delta\omega_{us}} d\mathbf{k} (B a_{\mathbf{k}}^\dagger + B^\dagger a_{\mathbf{k}})$, where $a_{\mathbf{k}}^\dagger$ is the creation operator for a photon with wave vector \mathbf{k} . The first and second integral cover narrow bandwidths $\Delta\omega_{ls}$ and $\Delta\omega_{us}$ centered around the lower and upper sideband respectively (see Sec. III A). The modes of the light field are treated as bath and are therefore traced out. Using the Born-Markov approximation, one obtains a master equation of standard Lindblad form (compare Eq. (2)). Collective Lamb shifts can be shown to be negligible in the setting considered here (see App. B 2). In the limit $t \rightarrow \infty$, this evolution drives the system into an entangled steady state. In the absence of noise and for $N \gg 1$,

$$\xi_\infty^{\text{ideal}} = (|\mu| - |\nu|)^2.$$

Next, we include additional processes such as thermal motion, undesired atomic transitions and fluctuating magnetic fields as well as resonant pump fields. Details can be found in Sec. III C. For large particle numbers $N_I = N_{II} = N \gg 1$ and $t \rightarrow \infty$, we find

$$\xi_\infty = \frac{1}{P_{2,\infty}} \frac{\tilde{\Gamma} + d\Gamma P_{2,\infty}^2 (|\mu| - |\nu|)^2}{\tilde{\Gamma} + d\Gamma P_{2,\infty}}, \quad (5)$$

where $P_{2,\infty}$ is the steady state value of the atomic polarization $P_2 = \frac{1}{N} \sum_{i=1}^N (|\uparrow\rangle_i \langle\uparrow| - |\downarrow\rangle_i \langle\downarrow|)$, Γ is the single particle decay rate and $\tilde{\Gamma}$ is the dephasing rate associated with noise effects. d is the optical depth of one atomic ensemble. As shown in Sec. III D, the application of resonant pump fields can be beneficial

even though noise is added by doing so. Note that for $d \rightarrow \infty$, $\xi_\infty \rightarrow \xi_\infty^{\text{ideal}}$. For a large optical depth, the entangling dynamics is significantly enhanced by collective effects. In contrast, noise processes are single particle effects and therefore not amplified by a factor d . Eq. (5) shows that for strong coupling between atoms and light, entanglement can be generated in a steady state. This is the main result of this article.

Intuitively, entanglement is created by virtue of interference of different processes in the first and second ensemble. As illustrated in Fig. 2, the interaction of light and atoms in the first ensemble is chosen such that the emission of a photon in the upper sideband corresponds to a spin flip $|\uparrow\rangle \rightarrow |\downarrow\rangle$. Similarly, the emission of a photon in the upper sideband involves a spin flip $|\downarrow\rangle \rightarrow |\uparrow\rangle$ in the second ensemble. Due to collective effects [11], light is emitted in forward direction with high probability, for hot samples with high optical depth. As spin flips in either ensemble lead to emission of light into the same spatial mode, both processes are indistinguishable if a photon is detected. (An analogous argument holds for photons in the lower sideband.) In this respect, the setup resembles quantum repeater schemes [2–10], where collective excitations in two atomic ensembles are converted to photons, which subsequently interfere at a 50/50 beamsplitter such that entanglement can be created conditioned on the detection of a photon in one of the two output ports of the beamsplitter [55]. Here, no beamsplitter is needed, since both ensembles emit into the same spatial mode. The most important difference, however, lies in the fact that our scheme is not conditioned on a specific measurement outcome. It works deterministically and does not require a detection of the emitted photon, as the measurement is performed continuously by the environment.

The ideas put forward in this work are devised and elaborated for two-level systems, but the proposed scheme can also be realized using atoms with multi-level ground states. The scheme put forward in this work has been realized recently [56] using alkali atoms. In this experiment, purely dissipatively driven entanglement between two macroscopic atomic ensembles at room temperature has been demonstrated yielding an order of magnitude improvement in the entanglement life time compared to previous experiments, where entanglement has been generated in this system using standard methods. In a multi-level setting, the population in the two-level subsystem is continually reduced due to undesired transitions to other ground state levels. We take this and other features of the multilevel structure into account and find that the continuous reduction of the collective spin leads to the production of a quasi steady state: the steady state with respect to the relevant two-level subsystem is superposed by slow additional dynamics due to the multi-level structure. This can be counteracted by the application of external pump fields.

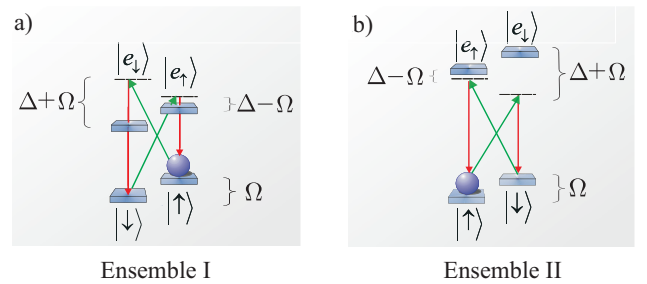


FIG. 2: (Color online) Atomic level schemes. a) A magnetic field which is oriented along \hat{x} (see Fig. 1) causes a Zeeman splitting Ω of atomic ground-states levels $|\uparrow\rangle$ and $|\downarrow\rangle$ and defines the quantization axis. A strong \hat{y} polarized coherent field with detuning Δ drives transitions $|\uparrow\rangle \rightarrow |e_\downarrow\rangle$ and $|\downarrow\rangle \rightarrow |e_\uparrow\rangle$. Coupling to the vacuum modes of the electromagnetic field gives rise to transitions $|e_\downarrow\rangle \rightarrow |\downarrow\rangle$ and $|e_\uparrow\rangle \rightarrow |\uparrow\rangle$. b) A static electric field is applied to the second ensemble such that the energy difference between ground and excited states is enhanced by 2Δ .

These fields add noise to the system and limit therefore the amount of entanglement that can be generated. However, for samples with high optical depth, incoherent pumping can render the creation of steady state entanglement in atoms with multi-level ground states possible. This is illustrated in Sec. IV B by considering ^{133}Cs vapors at room temperature and experimental parameters close to the values published in [49, 50, 56]. We take the most fundamental limitations imposed by undesired radiative processes into account and estimate that steady state entanglement with $\xi_\infty = 0.9$ should be attainable for a moderate optical depth $d = 30$ in the absence of other (implementation-dependent) sources of noise.

III. CREATION OF STEADY STATE ENTANGLEMENT IN A TWO-LEVEL SYSTEM

As outlined above, light modes act as environment and the interaction between the system and the reservoir is controlled by means of laser- and magnetic fields. In Sec. III A, we explain the interaction between atoms and light in more detail. The master equation governing the dissipative evolution of the reduced density matrix of the atomic system ρ is given by

$$d_t \rho = \mathcal{L}_{\text{ent}} \rho + \mathcal{L}_{\text{noise}} \rho,$$

where \mathcal{L}_{ent} and $\mathcal{L}_{\text{noise}}$ are Lindblad operators. Desired interactions give rise to the entangling dynamics represented by $\mathcal{L}_{\text{ent}} \rho$. The second term $\mathcal{L}_{\text{noise}} \rho$ summarizes all undesired effects.

Below, $\mathcal{L}_{\text{ent}} \rho$ and $\mathcal{L}_{\text{noise}} \rho$ are determined. To this end, the master equation corresponding to the light-matter interaction in Figs. 1 and 2 is derived in Sec. III B, including

undesired radiative processes. Excited states are adiabatically eliminated such that an effective master equation for atomic ground states $|\uparrow\rangle$ and $|\downarrow\rangle$ is obtained. In Sec. III C, thermal motion of atoms is taken into account and additional effects due to pump fields and noise processes are included. Based on these results, the amount of entanglement that can be produced is calculated in Sec. III D.

A. Light–matter interaction

In this subsection, we describe the setup for creation of entanglement between two atomic ensembles and explain how light and matter interact.

We consider the setup shown in Fig. 1. A strong $\hat{\mathbf{y}}$ -polarized laser beam propagates along $\hat{\mathbf{z}}$ and passes two atomic ensembles in a homogeneous magnetic field, which defines the quantization axis and is oriented along $\hat{\mathbf{x}}$. Each atomic ensemble consists of a large number N of hydrogen-like atoms with an internal level structure as depicted in Fig. 2. The laser field is assumed to cover a very narrow bandwidth b around the central frequency ω_L and to be off-resonant such that the interaction is well within the dispersive regime and absorption effects can be neglected. The detuning $|\Delta|$ is considered to be large compared to the Doppler width δ_{Doppler} and atomic decay rates Γ_{atomic} . Here and in the following, Γ_{atomic} denotes the largest effective atomic rate for transitions between ground state levels, including single particle as well as collective rates (see below). The magnetic field causes a Zeeman splitting of the atomic ground states Ω . The strong $\hat{\mathbf{y}}$ -polarized coherent beam is treated as classical field. With respect to quantization along $\hat{\mathbf{x}}$, it drives diagonal transitions $|\uparrow\rangle \rightarrow |e_{\downarrow}\rangle$, $|\downarrow\rangle \rightarrow |e_{\uparrow}\rangle$. Figs. 1 and 2 depict only desired transitions, where photons are scattered into the copropagating $\hat{\mathbf{x}}$ -polarized quantum field in two independent frequency bands, the upper and the lower sideband, centered around $\omega_L \pm \Omega$.

For the realization of the proposed scheme, several setups are possible. In a simple two-level model, where the Larmor splitting of excited states equals the Larmor splitting of ground states, a homogeneous static electric field can be applied to the second ensemble such that the resulting Stark shift enhances the energy difference between ground and excited states by 2Δ as shown in Fig. 2. This yields the following effective ground state Hamiltonian

$$H = H_A + H_L + H_{\text{int}},$$

where excited states have been eliminated under the condition $|\Delta| \gg \Gamma_{\text{atomic}}, \delta_{\text{Doppler}}$. Throughout the whole paper, the convention $\hbar \equiv 1$ is used. $H_A = \Omega(J_{x,I} - J_{x,II})$ accounts for the Zeeman splitting of atoms in the external magnetic field and $H_L = \int dk (\omega_k - \omega_L) a_k^\dagger a_k$ is the

free Hamiltonian of the light field. In a rotating frame, the interaction Hamiltonian is given by

$$\begin{aligned} H_{\text{int}} = & \int_{\Delta\omega_{ls}} d\mathbf{k} \sum_{\lambda_{\mathbf{k}}} \bar{g}(\mathbf{k}) \left(\mu \sum_{i=1}^N \sigma_{I,i} e^{i\Delta\mathbf{k}\mathbf{r}_i} + \nu \sum_{j=1}^N \sigma_{II,j}^\dagger e^{i\Delta\mathbf{k}\mathbf{r}_j} \right) a_{\mathbf{k}}^\dagger \\ & + \int_{\Delta\omega_{us}} d\mathbf{k} \sum_{\lambda_{\mathbf{k}}} \bar{g}(\mathbf{k}) \left(\mu \sum_{i=1}^N \sigma_{II,i} e^{i\Delta\mathbf{k}\mathbf{r}_i} + \nu \sum_{j=1}^N \sigma_{I,j}^\dagger e^{i\Delta\mathbf{k}\mathbf{r}_j} \right) a_{\mathbf{k}}^\dagger \\ & + H.C., \end{aligned} \quad (6)$$

where the first and second integral cover narrow bandwidths $\Delta\omega_{ls}$ and $\Delta\omega_{us}$ centered around the lower and upper sideband respectively. (A complete treatment based on the full Hamiltonian including all light modes can be found in App. B 1.) $\lambda_{\mathbf{k}}$ specifies the two orthogonal polarizations of the light mode with wave vector \mathbf{k} . The atomic operator $\sigma_{I/II,i} = |\uparrow\rangle_{I/II,i} \langle\downarrow|$ refers to a particle in ensemble I/II at position \mathbf{r}_i , $\Delta\mathbf{k} = \mathbf{k}_L - \mathbf{k}$, and \mathbf{k}_L is the wavevector of the applied classical field. AC Stark shifts have been absorbed in the detuning. $\bar{g}(\mathbf{k})\mu$ and $\bar{g}(\mathbf{k})\nu$ are the effective coupling strengths for the passive (beam splitter-like) part of the interaction and the active (squeezing) component of the Hamiltonian respectively. More specifically, $\bar{g}(\mathbf{k})\mu = \frac{\Omega_{\text{probe}}}{\Delta - \Omega} g_{\mathbf{k}}$ and $\bar{g}(\mathbf{k})\nu = \frac{\Omega_{\text{probe}}}{\Delta + \Omega} g_{\mathbf{k}}$, where Ω_{probe} is the Rabi frequency of the applied classical field. Here and in the following, we refer to the off-resonant (entangling) light field as probe field. In the following sections resonant fields are introduced which will be referred to as pump fields. The definition of the coupling constant for transitions between ground and excited states $g_{\mathbf{k}}$ can be found in App. B 1. The parameters $\mu = \frac{\Delta + \Omega}{2\sqrt{\Delta\Omega}}$ and $\nu = \frac{\Delta - \Omega}{2\sqrt{\Delta\Omega}}$ are normalized such that $\mu^2 - \nu^2 = 1$ [57].

A Hamiltonian of type (6) can be realized in many different ways. In general, the scheme presented here can be implemented in any system where a tunable quadratic interaction with an active and a passive part corresponding to two sideband modes can be realized, for example in ions or using optomechanical resonators. We focus here on the creation of dissipatively driven entanglement in atomic ensembles and continue considering the level structure depicted in Fig. 2. If the Larmor splitting of excited states is considerably larger than the splitting of ground states, it is for instance possible to introduce a $\lambda/2$ plate between the two ensembles instead of applying an external electric field [58]. As discussed in Sec. IV, alkali atoms provide another possibility to realize the desired light-matter interaction. Due to their multi-level structure it is not even necessary to introduce electric fields or passive optical elements.

We remark for clarity, that the possibility illustrated in Fig. 2 implies that the effective coupling constants (after adiabatic elimination) $\bar{g}(\mathbf{k})\mu$ and $\bar{g}(\mathbf{k})\nu$ describing the interaction of light with the first and the

second ensemble have different signs, as the light is blue detuned in the former and red detuned in the latter, such that $\mu_I = -\mu_{II}$ and $\nu_I = -\nu_{II}$. This is not the case in the implementation considered in Sec. IV. Due to the complex levels structure, both effective coupling constants have the same sign and therefore $\mu_I = \mu_{II}$ and $\nu_I = \nu_{II}$. In order to describe both alternatives in a compact way, we use a unified notation and absorb the sign in the definition of the atomic operators referring to the second ensembles $\sigma_{II,i} \rightarrow \text{sgn}(\mu_I \mu_{II}) \sigma_{II,i}$ as explained in App. B 2.

It is instructive to consider Hamiltonian (6), where excited levels have been adiabatically eliminated, because it shows clearly that the light matter interaction depicted in Fig. 2 corresponds to a beamsplitting interaction of the type $H \propto \int_{\Delta\omega_{ls}} d\mathbf{k} \left(A a_{\mathbf{k}}^\dagger + A^\dagger a_{\mathbf{k}} \right) + \int_{\Delta\omega_{us}} d\mathbf{k} \left(B a_{\mathbf{k}}^\dagger + B^\dagger a_{\mathbf{k}} \right)$ between photons in the upper and lower sideband with the nonlocal operators A and B (with additional phase factors $e^{\pm i\Delta\mathbf{k}\mathbf{r}_i}$). By deriving the corresponding master equation and including thermal motion as explained in Sec. III C, one can show that this Hamiltonian yields a master equation which consists of a desired part of type (2) with jump operators A and B and an additional contribution representing noise terms. However, in the following two subsections we derive the maser equation starting from the full Hamiltonian including excited levels since this approach is better suited to take dipole-dipole interactions into account.

B. Effective master equation for ground states

In the following, we outline the derivation of the master equation for atomic ground states $|\uparrow\rangle$ and $|\downarrow\rangle$ and comment on the approximations used to obtain the shown result. The full calculation can be found in App. B 1.

For brevity, we use a short hand notation and abbreviate master equations of Lindblad form $d_t \rho(t) = \kappa/2 (A\rho(t)A^\dagger - A^\dagger A\rho(t)) + H.C.$ with complex decay rate κ and jump operator A by the expression $\dot{\rho}(t) = \kappa/2 A\rho(t)A^\dagger + \dots$.

We consider the full Hamiltonian including excited levels and undesired transitions [59] without applying the rotating wave approximation for quantum fields (see Eq. B1). As explained in App. B1, counter-rotating terms play an important role in the calculation the imaginary parts of the master equation, but do not affect the real parts. Starting from the full Hamiltonian, we obtain a master equation of Lindblad form for the reduced atomic density matrix (see Eqs. (B2)-(B4)). To this end, we apply the approximation of independent rates of variation [60] and follow the standard procedure

assuming Born Markov dynamics. The approximation of independent rates of variations is valid if the Rabi frequency of the applied laser field Ω_{probe} is very small compared with the frequencies of atomic transitions. As we consider transitions in the optical domain, this assumption is clearly legitimate. More generally, here and in the following sections we consider situations exhibiting two very different time scales for variations in the system and in the bath of light modes $\Gamma_{\text{atomic}}\tau_c \ll 1$, where τ_c is the correlation time in the reservoir. For optical frequencies this is very well justified and we can therefore assume Born-Markov dynamics. Moreover, we restrict ourselves to settings, where the level splitting Ω between the states $|\uparrow\rangle$ and $|\downarrow\rangle$ is sufficiently large, such that the upper and lower sideband can be treated as independent baths [61] (compare App. B 1). Finally, we assume that the condition $k_L \gg R/L^2$ is fulfilled. k_L is the wave vector of the applied laser field. Since we consider frequencies in the optical domain, k_L is on the order of 10^7m^{-1} . L is the spatial extent of the atomic ensembles, which we consider to be on the order of cm, while the distance between the two ensembles R is about one meter.

As next step, excited states are adiabatically eliminated under the condition $|\Delta| \gg \Gamma_{\text{atomic}}, \delta_{\text{Doppler}}$. This leads to an effective master equation for atomic ground states. Using the abbreviated notation introduced in the beginning of this subsection,

$$\begin{aligned} d_t \rho(t) = & \frac{1}{2} \sum_{i,j=1}^N e^{-i\mathbf{k}_L(\mathbf{r}_j - \mathbf{r}_i)} J_{ij} \left(A_i \rho(t) A_j^\dagger + B_i \rho(t) B_j^\dagger \right) \\ & + \frac{1}{2} \sum_{i,j=1}^N e^{-i\mathbf{k}_L(\mathbf{r}_j - \mathbf{r}_i)} \check{J}_{ij} \left(C_i \rho(t) C_j^\dagger + D_i \rho(t) D_j^\dagger \right) \\ & + \dots \end{aligned} \quad (7)$$

where J_{ij} and \check{J}_{ij} are complex decay rates which are discussed below and $A = \frac{1}{\sqrt{N}} \sum_{i=1}^N A_i$. The operators B, C and D are analogously defined as sums. A_i, B_i, C_i and D_i are given by

$$\begin{aligned} A_i &= \mu \sigma_{I,i} + \nu \sigma_{II,i}^\dagger, \\ B_i &= \mu \sigma_{II,i} + \nu \sigma_{I,i}^\dagger, \\ C_i &= \mu \sigma_{\downarrow,I,i} + \nu \sigma_{\uparrow,II,i}, \\ D_i &= \mu \sigma_{\downarrow,II,i} + \nu \sigma_{\uparrow,I,i}, \end{aligned} \quad (8)$$

where the abbreviations $\sigma_{\uparrow,I/II,i} = |\uparrow\rangle_{I/II,i} \langle \uparrow|$ and $\sigma_{\downarrow,I/II,i} = |\downarrow\rangle_{I/II,i} \langle \downarrow|$ are used. Terms involving the operators A and B represent desired transitions involving a spin flip $|\uparrow\rangle \rightarrow |\downarrow\rangle$ or $|\downarrow\rangle \rightarrow |\uparrow\rangle$ as shown in Fig. 2. Terms involving the operators C or D represent undesired transitions which lead to dephasing [59]. Desired and undesired transitions are associated with different decay rates J_{ij} and \check{J}_{ij} respectively. In the four level model considered here, $\check{J}_{ij} = 2J_{ij}$, due to the ratio of

Clebsch Gordan coefficients $c_{\Delta_m=\pm 1}^2/c_{\Delta_m=0}^2 = 2$. As introduced above, $J_{ij} = \gamma(\mathbf{r}_{ij}) + ig(\mathbf{r}_{ij})$ is a complex decay rate with real part $\gamma(\mathbf{r}_{ij}) = \gamma(\mathbf{r}_{ji})$ and imaginary part $g(\mathbf{r}_{ij}) = g(\mathbf{r}_{ji})$. Imaginary single particle terms represent energy shifts (single atom Lamb shift) and are absorbed in the definition of detunings. Therefore we consider in the following only imaginary terms $g(\mathbf{r}_{ij})$ with $i \neq j$ and use renormalized atomic energies and the resulting effective detunings. The real and imaginary part of J_{ij} are given by [62]

$$\gamma(\mathbf{r}_{ij}) = \frac{3}{2}\Gamma \left(1 - (\hat{\mathbf{p}} \cdot \hat{\mathbf{r}}_{ij})^2\right) \frac{\sin(k_L r_{ij})}{k_L r_{ij}} \quad (9)$$

$$+ \frac{3}{2}\Gamma \left(1 - 3(\hat{\mathbf{p}} \cdot \hat{\mathbf{r}}_{ij})^2\right) \left(\frac{\cos(k_L r_{ij})}{(k_L r_{ij})^2} - \frac{\sin(k_L r_{ij})}{(k_L r_{ij})^3}\right),$$

$$g(\mathbf{r}_{ij}) = -\frac{3}{2}\Gamma \left(1 - (\hat{\mathbf{p}} \cdot \hat{\mathbf{r}}_{ij})^2\right) \frac{\cos(k_L r_{ij})}{k_L r_{ij}} \quad (10)$$

$$+ \frac{3}{2}\Gamma \left(1 - 3(\hat{\mathbf{p}} \cdot \hat{\mathbf{r}}_{ij})^2\right) \left(\frac{\sin(k_L r_{ij})}{(k_L r_{ij})^2} + \frac{\cos(k_L r_{ij})}{(k_L r_{ij})^3}\right),$$

where $\hat{\mathbf{p}}$ is the unit vector of the dipole matrix element $\mathbf{p} = \langle e_\uparrow | e \hat{\mathbf{x}} | \uparrow \rangle$, which we assume to be real. $\hat{\mathbf{r}}_{ij}$ is the unit vector of the interatomic distance $\mathbf{r}_{ij} = \mathbf{r}_i - \mathbf{r}_j$ and $r_{ij} = r_{ji}$ is the length of the vector \mathbf{r}_{ij} . Γ is the effective decay rate of a single isolated atom.

C. Master equation including thermal motion and noise processes

In this subsection, atomic motion is taken into account [63–65]. As is shown below, thermal motion gives rise to noise terms which are small compared the desired contributions for samples with high optical depth.

Atoms are statistically distributed. The dynamics of the whole system is thereby governed by two different time scales, the characteristic time of radiative emission $1/\Gamma_{\text{atomic}}$ and the characteristic time of atomic redistribution $\frac{L}{v}$, where L is the length of a cubic ensemble and v is the average velocity of particles. In the limit, where the time scale of atomic motion is fast compared to the time scale of radiative decay $\Gamma_{\text{atomic}} \frac{L}{v} \ll 1$ one can describe the emission independently of the evolution of atomic positions which enters the master equation in the form of averaged coefficients, where the average in time corresponds to an average in space [66]. Atomic positions can be treated as independent random variables and for simplicity, we choose a Gaussian probability distribution of width L , $P(r) = \frac{1}{\pi^{3/2} L^3} e^{-\frac{r^2}{L^2}}$ [65]. As shown in App. B, we find that imaginary parts of the averaged decay rates can be neglected. The averaged

master equation is given by

$$\begin{aligned} d_t \rho(t) &= \frac{1}{2} \sum_{i,j=1}^N \Gamma_{ij} \left(A_i \rho(t) A_j^\dagger + B_i \rho(t) B_j^\dagger \right) \\ &+ \frac{1}{2} \sum_{i,j=1}^N \check{\Gamma}_{ij} \left(C_i \rho(t) C_j^\dagger + D_i \rho(t) D_j^\dagger \right) \\ &+ \dots \end{aligned} \quad (11)$$

with $\check{\Gamma}_{ij} = 2\Gamma_{ij}$ for the basic model discussed here. For $k_L L \gg 1$ and $i \neq j$, $\Gamma_{ij} = \Gamma \frac{3}{4(k_L L)^2}$. $d = N \frac{\Gamma}{\Gamma_{ij}} = \frac{3N}{4(k_L L)^2}$ is the resonant optical depth of one atomic ensemble. Using this definition and $1/(k_L L)^2 \ll 1$, one obtains

$$\begin{aligned} d_t \rho(t) &= d \frac{\Gamma}{2} A \rho(t) A^\dagger + d \frac{\Gamma}{2} B \rho(t) B^\dagger \quad (12) \\ &+ \mu^2 \frac{\Gamma}{2} \sum_{i=1}^N \left(\sigma_{I,i} \rho(t) \sigma_{I,i}^\dagger + \sigma_{II,i} \rho(t) \sigma_{II,i}^\dagger \right) \\ &+ \nu^2 \frac{\Gamma}{2} \sum_{i=1}^N \left(\sigma_{I,i}^\dagger \rho(t) \sigma_{I,i} + \sigma_{II,i}^\dagger \rho(t) \sigma_{II,i} \right) \\ &+ d \frac{\check{\Gamma}}{2} C \rho(t) C^\dagger + d \frac{\check{\Gamma}}{2} D \rho(t) D^\dagger + \frac{\check{\Gamma}}{2} (\mu^2 + \nu^2) \\ &\sum_{i=1}^N \left(\sigma_{\downarrow\downarrow,I,i} \rho(t) \sigma_{\downarrow\downarrow,I,i} + \sigma_{\downarrow\downarrow,II,i} \rho(t) \sigma_{\downarrow\downarrow,II,i} \right) \\ &+ \dots \end{aligned}$$

The first three lines correspond to the first sum in Eq. (11). The entangling terms in the first line are enhanced by a factor d . For sufficiently optically thick samples, additional noise terms in the second and third line, which reflect thermal motion, are small compared to the desired contributions. The last two lines correspond to the second sum in Eq. (11), where $|\uparrow\rangle\langle\uparrow| + |\downarrow\rangle\langle\downarrow| = \mathbb{I}$ was used. The first two terms $d(\check{\Gamma}/2)C\rho(t)C^\dagger + d(\check{\Gamma}/2)D\rho(t)D^\dagger$ are collective dephasing terms. They do not have an effect on the entanglement generated (see App. C 2) and can therefore be omitted in the following.

In the following sections, the effect of pump fields is considered. Resonant pump fields cause incoherent cooling (and heating) processes, which can be taken into account by adding cooling (and heating) terms which correspond to a transfer of atoms from level $|\downarrow\rangle$ to level $|\uparrow\rangle$ (and back). Finally, we include additional processes, which do not lead to spin flips but cause dephasing, such as fluctuating magnetic fields. The full master equation

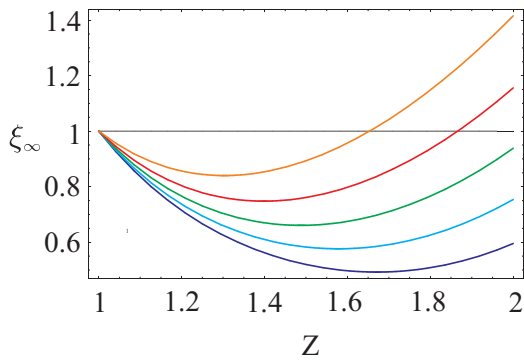


FIG. 3: (Color online) Steady state entanglement ξ_∞ in a two-level system versus $Z = (|\mu| - |\nu|)^{-1}$ for optical depth $d = 30$ per ensemble. The horizontal black line indicates the separable limit. (For separable states $\xi \geq 1$, the smaller ξ , the higher the amount of entanglement) The lowest line (violet) depicts ξ_∞ for purely radiative dephasing $\Gamma_d^{\text{add}} = 0$. The next curves show in ascending order $\Gamma_d^{\text{add}} = 2\Gamma$ (blue), $\Gamma_d^{\text{add}} = 5\Gamma$ (green), $\Gamma_d^{\text{add}} = 10\Gamma$ (red) and $\Gamma_d^{\text{add}} = 20\Gamma$ (orange), where Γ is the single particle decay rate.

is given by

$$\begin{aligned}
 d_t \rho(t) = & d \frac{\Gamma}{2} A \rho(t) A^\dagger + d \frac{\Gamma}{2} B \rho(t) B^\dagger \\
 & + \frac{\Gamma_{\text{cool}}}{2} \sum_{i=1}^N \left(\sigma_{I,i} \rho(t) \sigma_{I,i}^\dagger + \sigma_{II,i} \rho(t) \sigma_{II,i}^\dagger \right) \\
 & + \frac{\Gamma_{\text{heat}}}{2} \sum_{i=1}^N \left(\sigma_{I,i}^\dagger \rho(t) \sigma_{I,i} + \sigma_{II,i}^\dagger \rho(t) \sigma_{II,i} \right) \\
 & + \frac{\Gamma_d}{2} \sum_{i=1}^N \left(\sigma_{\downarrow\downarrow,I,i} \rho(t) \sigma_{\downarrow\downarrow,I,i} + \sigma_{\downarrow\downarrow,II,i} \rho(t) \sigma_{\downarrow\downarrow,II,i} \right) \\
 & + \dots
 \end{aligned} \tag{13}$$

Note that the last three lines represent single particle processes. They do not feature a collective enhancement factor d as the entangling terms in the first line. The noise terms proportional to $\Gamma\mu^2$ and $\Gamma\nu^2$ in the second and third line in expression (12) have been absorbed in lines two and three of Eq. (13). Hence, Γ_{cool} (Γ_{heat}) is the total single-particle cooling (heating) rate. Noise terms proportional to $\Gamma(\mu^2 + \nu^2)$ in expression (12) have been absorbed in the last line, such that Γ_d is the total dephasing rate. More details concerning the derivation of the full master equation (13) can be found in App. C 2.

D. Creation of entanglement

In this subsection, we determine how much entanglement can be generated by the proposed scheme in the presence of noise processes for a given optical depth d and given parameters μ and ν . Details of the calculation

can be found in App. C. For simplicity, we assume identical conditions for both ensembles. The amount of entanglement produced is measured by means of the quantity ξ defined in Eq. (3). Hence, the time evolution of $\Sigma_J = \text{var}(J_{y,I} + J_{y,II}) + \text{var}(J_{z,I} - J_{z,II})$ as well as the evolution of the mean value of the longitudinal spin $|\langle J_{x,I} \rangle| = |\langle J_{x,II} \rangle|$ need to be calculated. We consider the limit $N \gg 1$ and start by computing the former.

Σ_J decays according to

$$d_t \Sigma_J = - \left(\tilde{\Gamma} + d\Gamma P_2(t) \right) \Sigma_J + Nd\Gamma P_2(t)^2 (|\mu| - |\nu|)^2,$$

where $\tilde{\Gamma} = \Gamma_{\text{cool}} + \Gamma_{\text{heat}} + \Gamma_d$ and $P_2(t) = \frac{2}{N} \langle J_x \rangle$. The evolution of the mean value of the longitudinal spin is given by

$$d_t \langle J_x \rangle = -\frac{1}{2} (\Gamma_{\text{heat}} + \Gamma_{\text{cool}}) \langle J_x \rangle_t + \frac{N}{2} (\Gamma_{\text{cool}} - \Gamma_{\text{heat}}).$$

There are two distinct time scales. For atomic ensembles with high optical depth, the evolution of the transverse spin components is collectively enhanced and therefore fast compared to the decay of $\langle J_x \rangle$ which is due to single particle processes. In the limit where the entangled quantum state follows the changing atomic polarization adiabatically, the time evolution of $\xi(t)$ is given by

$$\begin{aligned}
 \xi(t) = & \frac{1}{P_2(t)} e^{-(\tilde{\Gamma} + d\Gamma P_2(t))t} \\
 & + \frac{1}{P_2(t)} \frac{\tilde{\Gamma} + d\Gamma P_2(t)^2 (|\mu| - |\nu|)^2}{\tilde{\Gamma} + d\Gamma P_2(t)} \left(1 - e^{-(\tilde{\Gamma} + d\Gamma P_2(t))t} \right).
 \end{aligned} \tag{14}$$

In the steady state

$$\begin{aligned}
 \xi_\infty = & \frac{1}{P_{2,\infty}} \frac{\tilde{\Gamma} + d\Gamma P_{2,\infty}^2 (|\mu| - |\nu|)^2}{\tilde{\Gamma} + d\Gamma P_{2,\infty}}, \\
 P_{2,\infty} = & \frac{\Gamma_{\text{cool}} - \Gamma_{\text{heat}}}{\Gamma_{\text{cool}} + \Gamma_{\text{heat}}}.
 \end{aligned} \tag{15}$$

This result shows that for high optical depth, the system reaches an entangled steady state. Under the dissipative dynamics considered here, entanglement persists for arbitrarily long times. In the absence of noise, $\tilde{\Gamma} = 0$ and Eq. (15) reduces to $\xi_\infty = (|\mu| - |\nu|)^2$.

Fig. 3 shows the attainable amount of entanglement in the steady state ξ_∞ for moderate optical depth $d = 30$ versus $Z = (|\mu| - |\nu|)^{-1}$ if only probe fields are applied. In this case $\Gamma_{\text{cool}}^{\text{probe}} = \mu^2\Gamma$ and $\Gamma_{\text{heat}}^{\text{probe}} = \nu^2\Gamma$. The dephasing rate $\Gamma_d = \Gamma_d^{\text{rad}} + \Gamma_d^{\text{add}}$ consists of a radiative part $\Gamma_d^{\text{rad,probe}} = 2(\mu^2 + \nu^2)\Gamma$ [67], which is due to light-induced transitions $|\uparrow\rangle \rightarrow |\uparrow\rangle$ and $|\downarrow\rangle \rightarrow |\downarrow\rangle$, and an additional term Γ_d^{add} which summarizes all non-radiative sources of dephasing such as fluctuating magnetic fields. This additional component can take values up to $\Gamma_d^{\text{add}} = 20\Gamma$ while still allowing for a reduction of ξ_∞ by 15%. For large

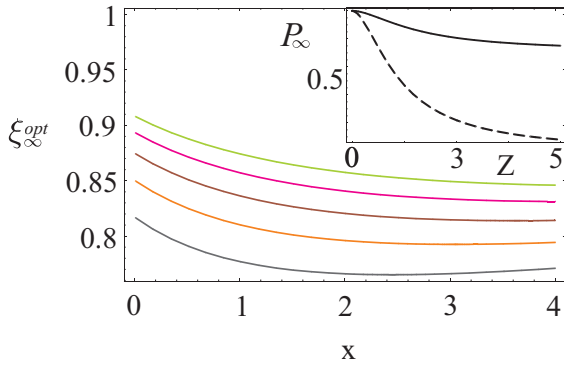


FIG. 4: (Color online) Steady state entanglement $\xi_{\infty}^{\text{opt}}$ for optimal squeezing parameter Z versus pump parameter x . (Two-level model, $d = 30$). The curves correspond in ascending order to $\Gamma_d^{\text{add}} = 15\Gamma$ (grey), $\Gamma_d^{\text{add}} = 20\Gamma$ (orange), $\Gamma_d^{\text{add}} = 25\Gamma$ (brown), $\Gamma_d^{\text{add}} = 30\Gamma$ (pink) and $\Gamma_d^{\text{add}} = 35\Gamma$ (light green). The inset shows the steady state polarization $P_{2,\infty}$ versus Z in the absence of pump fields $x = 0$ (dashed line) and for $x = 5$ (solid line).

values of Γ_d^{add} , the limiting mechanism is the decrease in polarization for high squeezing parameters and can be counteracted by applying resonant σ_+ and σ_- polarized pump fields to the first and second ensemble respectively, which drive the transition $|\downarrow\rangle \rightarrow |e_{\uparrow}\rangle$. In this case, the cooling rate can be roughly estimated as $\Gamma_{\text{cool}} = (1+x)\Gamma\mu^2$ [68]. The pump parameter x is given by $x = \frac{\Omega_{\text{pump}}^2 (\Delta - \Omega)^2}{\gamma_{\text{LW}}^2 \Omega_{\text{probe}}^2} k$, where Ω_{pump} is the Rabi frequency of the pump field and γ_{LW} is the natural line width of excited levels. The correction factor k takes Doppler broadening due to thermal motion into account [69]. In the presence of pump fields, radiative dephasing is enhanced $\Gamma_d^{\text{rad}} = 2((1+x)\mu^2 + \nu^2)\Gamma$. The heating rate is unaffected. Fig. 4 shows the maximal attainable amount of entanglement $\xi_{\infty}^{\text{opt}}$ (entanglement for optimal squeezing parameter Z), for $d = 30$ versus pump parameter x . For $x = 5$, additional dephasing up to $\Gamma_d^{\text{add}} = 37\Gamma$ can be tolerated while still allowing for a reduction of $\xi_{\infty}^{\text{opt}}$ by 15%. Remarkably, the application of external pump fields, which amounts to adding extra noise to the system, is advantageous in this case.

IV. IMPLEMENTATION IN MULTI-LEVEL SYSTEMS

In Sec. III, the theoretical framework for creating steady state entanglement between two atomic ensembles at room temperature is presented in detail for two-level systems. This section complements the main results derived in Sec. III by considering the implementation in multi-level systems. In the following we investigate the possibility of transferring the concepts developed for two-level systems to atoms with multi-level ground

states by means of a general simplified model and analyze the conditions for obtaining entanglement in a steady state qualitatively.

As specific example, we study the implementation of the proposed scheme in ensembles of alkali atoms, where the two-level system is encoded in a multi-level ground state manifold. Due to the richer internal structure, no external electric fields or optical elements need to be employed in contrast to the setup discussed in the previous section. As explained below, suitable values $\mu_I = \mu_{II}$ and $\nu_I = \nu_{II}$ are realized naturally. In principle, it is possible to include all magnetic sublevels and all possible transitions of a particular alkali atom in the following consideration. However, rather than aiming for a complete description which takes the entire level structure of a specific atom into account, the general model used here is primarily intended to describe the underlying physics. In Sec. IV A, we show how additional dynamics in a multi-level system can be taken into account by means of this simplified model which allows us to describe the physical effects with a small set of parameters while capturing all relevant features. In Sec. IV B we estimate the attainable entanglement.

A. Including multi-level dynamics

In the following we consider encoding of a two-level subsystem in a multi-level ground state. For example, the ground state of alkali atoms with nuclear spin I is split in two manifolds with total angular momentum $F = I + 1/2$ and $F' = I - 1/2$ respectively. The relevant two-level subsystem can be encoded in the two outermost states of the $F = I + 1/2$ ground state manifold $|\uparrow\rangle \equiv |F, \pm F\rangle$ and $|\downarrow\rangle \equiv |F, \pm(F-1)\rangle$ in the first/second ensemble.

In general, the maximum attainable amount of entanglement $\xi^{\text{ideal}} = (|\mu| - |\nu|)^2$ is determined by the different rates $\mu^2\Gamma$ and $\nu^2\Gamma$ at which probe-field induced transitions $|\downarrow\rangle \rightarrow |\uparrow\rangle$ and $|\uparrow\rangle \rightarrow |\downarrow\rangle$ occur. The values of the parameters μ and ν depend on the multi-level structure of the excited states as well as on polarization and detuning of the applied laser field. This can be illustrated by considering the off-resonant probing of ^{133}Cs atoms on the D_2 line using the setup shown in Fig. 1. \hat{y} -polarized probe light which propagates along \hat{z} , interacts successively with two Cs ensembles in \hat{x} -oriented magnetic fields. We assume weak magnetic fields ($B \approx 1\text{Gauss}$), such that the Larmor splitting $\Omega \approx 300\text{kHz}$ is much smaller than the fine splitting of excited states. The first ensemble is strongly spin polarized along the orientation of the magnetic field, while the second ensemble is polarized antiparallel. As shown in Fig. 5, the passive interaction, which transfers atoms from $|\downarrow\rangle$ to $|\uparrow\rangle$ involves the upper levels with $F = 4, 5$, whereas the active part of the light-matter interaction $|\uparrow\rangle \rightarrow |\downarrow\rangle$ involves the manifolds with

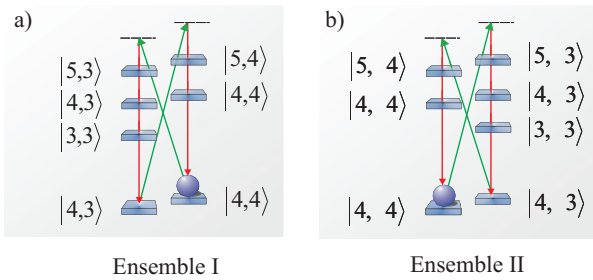


FIG. 5: (Color online) Implementation of the proposed scheme in ^{133}Cs ensembles. The atomic samples are placed in \hat{x} polarized magnetic fields and interact with a \hat{y} polarized probe field propagating along \hat{z} as shown in Fig. 1. The relevant two-level subsystem is encoded in the $6S_{1/2}$ ground state, $|\uparrow\rangle \equiv |4, \pm 4\rangle$ and $|\downarrow\rangle \equiv |4, \pm 3\rangle$ in the first/second ensemble and are coupled to the excited states in $6P_{3/2}$. Only desired transitions are shown. Level splittings are not represented true-to-scale. (In a magnetic field of 1 Gauss, the Zeeman shift of magnetic sublevels is about 10^5 Hz while the hyperfine, -and fine splitting is on the order of 10^8 Hz and 10^{14} respectively.)

$F = 3, 4, 5$. Taking the different Clebsch Gordan coefficients into account, one obtains $Z = (\mu - \nu)^{-1} = 2.3$ for blue detuning $\Delta = 700$ MHz with respect to the $F = 5$ manifold of $6P_{3/2}$. (Both parameters, μ and ν , are positive.) Alternatively, \hat{x} polarized probe light can be used in combination with red detuning as shown in Fig. 6. In this case $Z = 2.4$ for $\Delta = -700$ MHz. Both variants are possible; in the following we will consider \hat{x} polarized probe fields.

More generally, the multi-level structure of excited states affects only the value of ξ^{ideal} . The multi-level character of the ground state leads to additional dynamics that needs to be taken into account. Firstly, atoms can leave the relevant two-level subsystem. While matter and light interact, atoms redistribute or are lost to other groundstate manifolds. Therefore, the atomic population in the two-level subsystem is continually reduced. This is accounted for by introducing a time dependent population $N_2(t)$ and including the effect accordingly in the corresponding polarization $P_2(t)$. The subscript "2" emphasizes that these quantities are defined with respect to the two-level subsystem $\{|\uparrow\rangle, |\downarrow\rangle\}$. In order to calculate $N_2(t)$ and $P_2(t)$ in Sec. IV B, we introduce now a general model which allows one to analyze the realization of the proposed scheme in atoms with multi-level ground states. A high degree of population and polarization with respect to the two-level subsystem is required in the process of generating long-lived entanglement. Therefore σ_{\pm} polarized pump and repump fields have to be applied. These additional fields induce transitions with $\Delta m_F = +1$ in the first ensemble and transitions with $\Delta m_F = -1$ in the second one. For alkali ensembles, pump fields drive transitions

within the manifold $F = I + 1/2$ while repump fields transfer atoms in $F' = I - 1/2$ back to $F = I + 1/2$. In the desired case of high polarization with respect to the two outermost states, the atomic population in sublevels with $F = 4, \pm m_F < 3$ in the first/second ensemble can be neglected. In this regime it is sufficient to restrict the description to three states, $|\uparrow\rangle, |\downarrow\rangle$ and $|h\rangle \equiv |F', F'\rangle$ for the first and $|h\rangle \equiv |F', -F'\rangle$ for the second ensemble, as shown in Fig. 6.

Finally, one has to distinguish between spin operators which refer to the relevant two-level subsystem and experimentally measurable quantities which are defined with respect to $F = I + 1/2$. For clarity, operators referring to the full multi-level structure are labelled with the subscript "exp". The longitudinal spin of each ensemble is given by

$$\begin{aligned} J_{x,\text{exp}} &= \sum_{i=1}^N \sum_{m=-F}^F m |m\rangle_i \langle m| \\ &\approx \sum_{i=1}^N (F|\uparrow\rangle_i \langle \uparrow| + (F-1)|\downarrow\rangle_i \langle \downarrow|) \\ &= J_{x,2} + \frac{2F-1}{2} N_2(t), \end{aligned} \quad (16)$$

where $N_2 = \sum_{i=1}^N (|\uparrow\rangle_i \langle \uparrow| + |\downarrow\rangle_i \langle \downarrow|)$. For transverse spin components,

$$\begin{aligned} J_{y,\text{exp}} &= \frac{1}{2} \sum_{i=1}^N \sum_{m=-F}^F \sqrt{F(F+1) - m(m+1)} (|m+1\rangle_i \langle m| \\ &\quad + |m\rangle_i \langle m+1|) \approx \sqrt{2F} J_{y,2}, \end{aligned} \quad (18)$$

such that

$$\Sigma_{J,\text{exp}} = 2F \Sigma_{J,2} + 2(2F-1) N_{\downarrow}, \quad (19)$$

with $N_{\downarrow} = \sum_{i=1}^N |\downarrow\rangle_i \langle \downarrow|$.

B. Dissipatively driven entanglement between two alkali ensembles

In the following, we outline the calculation of the entanglement which can be produced in the described setting and compute the time evolution of $\xi_{\text{exp}}(t)$. The master equation governing the evolution of the atomic system according to the general model outlined in Sec. IV A, as well as details of the calculation summed up below, can be found in App. D.

Atomic populations $N_{\uparrow} = \sum_{i=1}^N |\uparrow\rangle_i \langle \uparrow|$, $N_{\downarrow} = \sum_{i=1}^N |\downarrow\rangle_i \langle \downarrow|$ and $N_h = \sum_{i=1}^N |h\rangle_i \langle h|$ can be calculated using the rate equations

$$d_t \begin{pmatrix} N_{\uparrow}(t) \\ N_{\downarrow}(t) \\ N_h(t) \end{pmatrix} = M \begin{pmatrix} N_{\uparrow}(t) \\ N_{\downarrow}(t) \\ N_h(t) \end{pmatrix}, \quad (20)$$

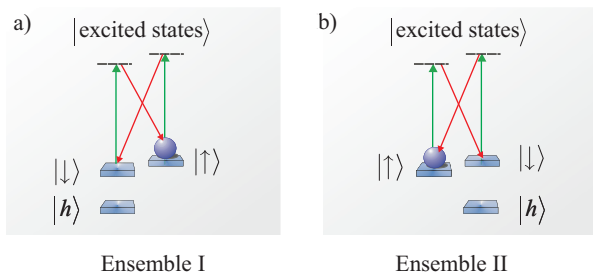


FIG. 6: (Color online) General scheme for the realization of long-lived entanglement between alkali-ensembles. The polarization of the probe field is assumed to be parallel to the applied magnetic field. The ground state $S_{1/2}$ consists of two manifolds with total spin $F = I + 1/2$ and $F' = I - 1/2$, where I is the nuclear spin. The states $|\uparrow\rangle$ and $|\downarrow\rangle$ are encoded in the outermost levels of the $F = I + 1/2$ ground state manifold. We identify $|\uparrow\rangle \equiv |F, F\rangle$ and $|\downarrow\rangle \equiv |F, F - 1\rangle$ for the first atomic ensemble and $|\uparrow\rangle \equiv |F, -F\rangle$ and $|\downarrow\rangle \equiv |F, -F + 1\rangle$ for the second one. Only desired transitions are shown. In the presence of strong pump fields, the amount of entanglement generated can be estimated by a simplified three level model including the state $|h\rangle \equiv |F', \pm F'\rangle$, for the first/second ensemble.

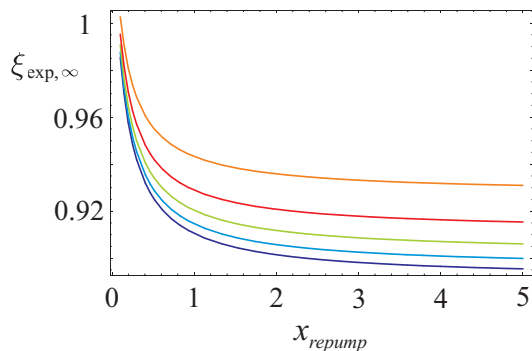


FIG. 7: (Color online) Steady state entanglement $\xi_{\text{exp},\infty}$ between two ^{133}Cs ensembles versus strength of repump fields x_{repump} (see main text, Sec. IV B and App. E). The plots depict data for ensembles with optical depth $d = 30$, blue detuned probe light with $\Delta = 700\text{MHz}$ and different values for the non-radiative dephasing rate Γ_d^{add} . The curves correspond in ascending order to $\Gamma_d^{\text{add}} = 0$ (violet), $\Gamma_d^{\text{add}} = 2$ (blue), $\Gamma_d^{\text{add}} = 5$ (green), $\Gamma_d^{\text{add}} = 10$ (red) and $\Gamma_d^{\text{add}} = 20$ (orange).

where

$$M = \begin{pmatrix} -(\Gamma_{\uparrow\downarrow} + \Gamma_{\uparrow h}) & \Gamma_{\uparrow\downarrow} & \Gamma_{h\uparrow} \\ \Gamma_{\uparrow\downarrow} & -(\Gamma_{\uparrow\downarrow} + \Gamma_{\downarrow h}) & \Gamma_{h\downarrow} \\ \Gamma_{\uparrow h} & \Gamma_{\downarrow h} & -2(\Gamma_{h\uparrow} + \Gamma_{h\downarrow}) \end{pmatrix}.$$

Γ_{ab} is the single-particle rate for the transition $|a\rangle \rightarrow |b\rangle$. If the transition rates are known, the number of atoms in the relevant two-level subsystem $N_2(t) = N_{\uparrow} + N_{\downarrow}$ and the polarization $P_2(t) = (N_{\uparrow} - N_{\downarrow})/N_2(t)$ can be

directly computed. Based on this result, the time evolution of $\Sigma_{J,2} = \text{var}(J_{y,I} + J_{y,II})_2 + \text{var}(J_{z,I} - J_{z,II})_2$ can be calculated. Again, the situation exhibits two different time scales. The decay collective of $\Sigma_{J,2}$ is fast compared to the evolution of $N_2(t)$ and $P_2(t)$. A calculation analogous to the one described in App. C leads to

$$\begin{aligned} \Sigma_{J,2} &= N_2(0)e^{-(\bar{\Gamma} + d(t)\Gamma P_2(t))t} \\ &+ N_2(t) \frac{\bar{\Gamma} + d(t)\Gamma P_2(t)^2 (\mu - \nu)^2}{\bar{\Gamma} + d(t)\Gamma P_2(t)} \\ &\left(1 - e^{-(\bar{\Gamma} + d(t)\Gamma P_2(t))t}\right), \end{aligned} \quad (21)$$

with $d(t) = dN_2(t)/N$ and $\bar{\Gamma} = \Gamma_{\uparrow\downarrow} + \Gamma_{\uparrow\downarrow} + \Gamma_{\uparrow h} + \Gamma_{\downarrow h} + \Gamma_{\uparrow\uparrow} + \Gamma_{\downarrow\downarrow} + \Gamma_d^{\text{add}}$, where Γ_d^{add} accounts for non-radiative dephasing. On time scales which are long compared to the fast desired dynamics (but short enough to avoid profuse depletion of the relevant two-level subsystem, such that $N_2(t) \gg 1$ is guaranteed) $\Sigma_{J,2}$ is given by the long-time (lt) solution

$$\Sigma_{J,2}^{\text{lt}} = N_2(t) \frac{\bar{\Gamma} + d(t)\Gamma P_2(t)^2 (\mu - \nu)^2}{\bar{\Gamma} + d(t)\Gamma P_2(t)}. \quad (22)$$

Now, this result is related to experimentally measurable quantities. Inserting Eqs. (17), (18), (19) and (22) into the definition $\xi_{\text{exp}} = \Sigma_{J,\text{exp}} / (2 | \langle J_x \rangle_{\text{exp}} |)$ yields

$$\begin{aligned} \xi_{\text{exp}}^{\text{lt}} &= \frac{\bar{\Gamma} + d(t)\Gamma P_2(t)^2 (\mu - \nu)^2}{\bar{\Gamma} + d(t)\Gamma P_2(t)} \frac{2F}{P_2(t) + 2F - 1} \\ &+ \frac{N_{\downarrow}(t)}{N_2(t)} \frac{2(2F - 1)}{P_2(t) + 2F - 1}. \end{aligned} \quad (23)$$

This long-time solution is a generalization of Eq. (5) which takes multi-level dynamics into account. Particle losses result in a decrease in $d(t)$ and $P_2(t)$. If transitions out of the two-level subsystem can be counteracted efficiently by pump- and repump-fields, a true entangled steady state can be reached. Else, a quasi steady state is produced. These two cases are illustrated in Figs. 7 and 8 respectively using the concrete example of ^{133}Cs ensembles ($F=4$) at room temperature. Fig. 7 shows the amount of steady state entanglement generated in case of sufficient repump power. More specifically, the depicted curves represent solutions for different values of Γ_d^{add} versus the repump parameter x_{repump} , starting from $x_{\text{repump}} = 0.01$. The repump parameter x_{repump} quantifies the strength of the applied repump fields and is given by the ratio $x_{\text{repump}} = \Omega_{\text{repump}}^2 / \Omega_{\text{pump,opt}}^2$, where $\Omega_{\text{pump,opt}}^2$ is the optimal Rabi frequency that can be chosen for the pump field within the validity of the model considered here. ($\Omega_{\text{pump,opt}}^2$ is the minimal Rabi frequency of the pump field leading to $N_{\uparrow,\infty}/N_{2,\infty} \geq 0.95$ in the steady state.) Details of the calculations leading to the plots can be found in App. E. Fig. 8 illustrates the case, where particle losses dominate the evolution of $\xi_{\text{exp}}(t)$. The curves in this figure show the amount of entanglement generated in the absence of repump fields

as a function of time in ms. For short times the time evolution is governed by the desired dynamics within the relevant two-level subsystem and reaches quickly an entangled steady state. For longer times this stable state with respect to the entangling dynamics is superposed by the slow additional evolution imposed by the multi-level structure of the ground state. The fast desired dynamics entangles the collective spins of both ensembles, while particle losses cause a slow but continuing shortening of the spins. In this sense, Fig. 8 shows the creation of a quasi steady state. For $t > 0.05/\Gamma$, the time evolution is given by Eq. (23), that is, the time evolution is solely determined by particle loss-related dynamics.

In this section, we put emphasis on the general, implementation-independent limitations of the proposed scheme imposed by radiative transitions. These undesired processes are characteristic for a given level scheme and intimately linked to the tradeoff between enhanced entangling dynamics due to increased probe- or pump power and added noise. Depending on the concrete experimental realization, other undesired processes impairing the performance of the proposed scheme can occur like for example spin flips due to collisions. Atomic transitions and additional dephasing due to collisions with the walls can be taken into account by including terms of the type

$$\begin{aligned} d_t \rho(t) = & \frac{\Gamma_{\text{col}}}{2} \sum_{i=1}^N \left(\sigma_{I,i} \rho(t) \sigma_{I,i}^\dagger + \sigma_{II,i} \rho(t) \sigma_{II,i}^\dagger \right) \\ & + \frac{\Gamma_{\text{col}}}{2} \sum_{i=1}^N \left(\sigma_{I,i}^\dagger \rho(t) \sigma_{I,i} + \sigma_{II,i}^\dagger \rho(t) \sigma_{II,i} \right) \\ & + \frac{\Gamma_{\text{col}}}{2} \sum_{i=1}^N \left(\sigma_{\downarrow,I,i} \rho(t) \sigma_{\downarrow,I,i} + \sigma_{\downarrow,II,i} \rho(t) \sigma_{\downarrow,II,i} \right) \\ & + \dots \end{aligned}$$

to the master equation. Since the thermal energy of atoms is typically much larger than the atomic level splittings, one can assume the same collisional rate Γ_{col} for all atomic transitions. The value of Γ_{col} has to be determined phenomenologically for the specific experimental setup under consideration (compare [56]).

V. CONCLUSIONS

In conclusion, we propose a technique for entangling two mesoscopic atomic ensembles at room temperature which are separated by a macroscopic distance. The core idea is to engineer the coupling of the atomic system to its environment in such a way that the steady state of the dissipative time evolution is the desired inseparable state. As entanglement is produced in the steady state of the system, it is long-lived and immune to noise. The reservoir consists of the common modes of the electromagnetic field and the coupling of the bath to

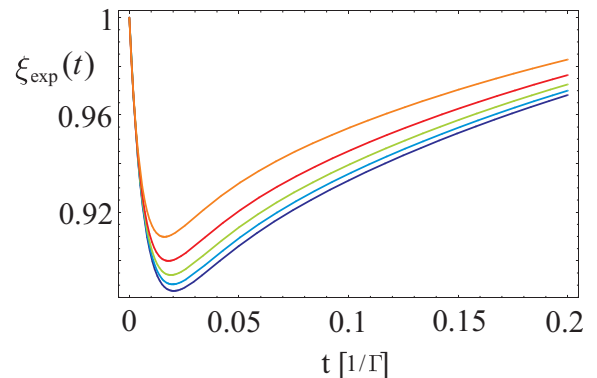


FIG. 8: (Color online) Quasi steady state entanglement of ^{133}Cs ensembles versus time in units $1/\Gamma$ in the absence of repump fields ($x_{\text{repump}} = 0$; all other parameters take values as in Fig. 7). The fast entangling dynamics results in a drop in $\xi_{\text{exp}}(t)$ (indicating the creation of an inseparable state), but since particle losses are not counteracted by repump-fields, this additional slow dynamics eventually causes $\xi_{\text{exp}}(t)$ to rise. Hence, a quasi steady state is produced. The behavior on long time scales is determined by the stationary state given by Eq. (15) superposed by slow multi-level dynamics.

the system can be controlled by means of laser- and magnetic fields. We provide a detailed theoretical description including dipole-dipole interactions for two-level systems and find that the imaginary parts of the master equation (collective Lamb shifts) are negligible. Hence, light-induced collisions do not play an important role in the setup considered here. The proposed scheme for generation of entanglement by dissipation is analyzed for two level systems and complemented by considering the implementation in multi-level ground states.

Future directions include the transfer of the ideas presented here to other systems, where a quadratic interaction involving two sideband modes can be realized. The system may either be described by bosonic modes (compare Sec. II and App. A) or spin degrees of freedom. If the Hamiltonian corresponding to the interaction between this system and light can be decomposed into an active and a passive part such that each part involves one sideband, as in Hamiltonian (6), dissipatively driven entanglement can be generated using the method described in this paper.

Optomechanical resonators [81–83] interacting with light are promising candidates. If an optomechanical system is driven by a strong pump laser, the linearized radiation-pressure Hamiltonian gives rise to a passive (beam-splitter) interaction for positive detuning between cavity and pump-frequency [84, 85]. The resulting effective interaction is active (squeezing) for negative detuning. The effective optomechanical coupling rates can be adjusted by tuning the intensities of the driving

fields [86]. Hence, the quadratic interaction in this system provides naturally the basic prerequisites for implementation of the proposed scheme. One can for example envision a setup, where light interacts subsequently with two movable mirrors which each constitute one end of an optical cavity such that the nanomechanical oscillators are driven into an entangled state. Equivalently, membranes coupled to Fabri-Perot cavity modes could be used.

Acknowledgements

We thank Geza Giedke, Karl Gerd Vollbrecht, Klemens Hammerer, Markus Aspelmeyer and Diego Porras for very valuable discussions and express our gratitude to Hanna Krauter, Kasper Jensen and Wojciech Wasilewski for their input concerning the implementation of the proposed scheme in Cesium vapor cells. We acknowledge support from the Elite Network of Bavaria (ENB) project QCCC, the DFG-Forschungsgruppe 635 and the EU projects COMPAS, Q-ESSENCE and QUE-VADIS.

Appendix A: Steady state entanglement for bosonic modes

In the following, it is shown that the two mode squeezed state $\rho_{\text{TMS}} = |\Psi_{\text{TMS}}\rangle\langle\Psi_{\text{TMS}}|$, with $\tilde{A}|\Psi_{\text{TMS}}\rangle = \tilde{B}|\Psi_{\text{TMS}}\rangle = 0$, is the unique steady state of the time evolution described by the Master equation

$$d_t\rho(t) = \kappa_A \left(\tilde{A}\rho(t)\tilde{A}^\dagger - \tilde{A}^\dagger\tilde{A}\rho(t)/2 - \rho(t)\tilde{A}^\dagger\tilde{A}/2 \right) + \kappa_B \left(\tilde{B}\rho(t)\tilde{B}^\dagger - \tilde{B}^\dagger\tilde{B}\rho(t)/2 - \rho(t)\tilde{B}^\dagger\tilde{B}/2 \right).$$

As stated in Sec. II, the bosonic mode operators a and b ($[a, a^\dagger] = [b, b^\dagger] = 1$) can be transformed into the non-local operators \tilde{A} and \tilde{B} by the unitary operation

$$\begin{aligned} \tilde{A} &= UaU^\dagger = \mu a + \nu b^\dagger, \\ \tilde{B} &= UbU^\dagger = \mu b + \nu a^\dagger. \end{aligned}$$

Since unitary transformations preserve commutation relations, $[\tilde{A}, \tilde{A}^\dagger] = [\tilde{B}, \tilde{B}^\dagger] = 1$ with $\mu^2 - \nu^2 = 1$. By inserting these expressions in the equation above and defining $\rho_U = U^\dagger\rho U$ we find

$$d_t\rho_U(t) = \kappa_A (a\rho_U(t)a^\dagger - a^\dagger a\rho_U(t)/2 - \rho_U(t)a^\dagger a/2) + \kappa_B (b\rho_U(t)b^\dagger - b^\dagger b\rho_U(t)/2 - \rho_U(t)b^\dagger b/2). \quad (\text{A1})$$

This is a master equation for two modes coupled to a bath with temperature $T = 0$. The steady state is the vacuum $|0, 0\rangle\langle 0, 0|$, with $a|0, 0\rangle = b|0, 0\rangle = 0$ [70]. Hence, inverting the unitary transformation yields the unique steady state $U|0, 0\rangle = |\Psi_{\text{TMS}}\rangle$.

For bosonic modes, the amount of entanglement can be quantified by means of the violation of a local uncertainty relation in terms of quadratures [71, 72]. For entangled states

$$\text{var}(x_+) + \text{var}(p_-) < 1,$$

where $x_+ = (x_a + x_b)/\sqrt{2}$, $p_- = (p_a - p_b)/\sqrt{2}$ and $x_a = (a + a^\dagger)/\sqrt{2}$ and $p_a = -i(a - a^\dagger)/\sqrt{2}$ (analogous expressions hold for x_b and p_b). In particular, $\text{var}(x_+) + \text{var}(p_-) = (\mu - \nu)^{-2} = e^{-2r}$, for two mode squeezed states with squeezing parameter r .

For large, strongly polarized atomic ensembles, collective spins can be described by bosonic modes $\frac{1}{\sqrt{N_I}} \sum_{i=1}^{N_I} \sigma_{I,i} \approx a$, $\frac{1}{\sqrt{N_{II}}} \sum_{i=1}^{N_{II}} \sigma_{II,i} \approx b$ using the Holstein-Primakoff-approximation [73]. In this case, $\xi < 1$ (see Sec. II) is equivalent to the criterion $\text{var}(x_+) + \text{var}(p_-) < 1$.

Appendix B: Derivation of the master equation

In this appendix, the master equation for creating entanglement between two atomic ensembles at room temperature discussed in Sec. III, is derived in detail. App. B 1 and App. B 2 complement Sec. III B and Sec. III C respectively. In the former, we derive the master equation for atomic ground states, Eq. (B5). In the latter, we include thermal motion of atoms and calculate the effective decay rates. We show that in the setup under consideration, the resulting master equation can be assumed to be real, since imaginary parts play only a minor role.

1. Master equation for atomic ground state levels $|\uparrow\rangle$ and $|\downarrow\rangle$

Light and matter are assumed to interact as described in Sec. III A. We consider the full Hamiltonian including undesired transitions [59] and without applying the rotating wave approximation for quantum fields. It is given by $H = H_L + H_A + H_{\text{int}}$, where $H_L = \int dk (\omega_k - \omega_L) a_k^\dagger a_k$ is the Hamiltonian of the free light field and H_A accounts for atomic energies in the rotating frame. $H_A = H_{A,I} + H_{A,II}$ with $H_{A,I} = \sum_i (\Delta_{\uparrow,I} |e_\uparrow\rangle_{I,i} \langle e_\uparrow| + \Delta_{\downarrow,I} |e_\downarrow\rangle_{I,i} \langle e_\downarrow|)$ and $H_{A,II} = \sum_i (\Delta_{\uparrow,II} |e_\uparrow\rangle_{II,i} \langle e_\uparrow| + \Delta_{\downarrow,II} |e_\downarrow\rangle_{II,i} \langle e_\downarrow|)$. Here, we introduced the detunings $\Delta_{\uparrow,I/II}$ and $\Delta_{\downarrow,I/II}$ which correspond to diagonal transitions $|\downarrow\rangle \rightarrow |e_\uparrow\rangle$ and $|\uparrow\rangle \rightarrow |e_\downarrow\rangle$ respectively in the first/second ensemble. In the setup illustrated in Fig. 2, $\Delta_{\uparrow,I} = -\Delta_{\uparrow,II} = \Delta - \Omega$ and $\Delta_{\downarrow,I} = -\Delta_{\downarrow,II} = \Delta + \Omega$. The interaction Hamiltonian $H_{\text{int}} = H_{\text{cl}} + H_{\text{qu}}$ consists of a classical part H_{cl} , which accounts for transitions induced by the driving field and a quantum part H_{qu} , which involves quantized field operators. The Hamiltonian describing the interaction of light with the first atomic ensemble is governed

by the Hamiltonian

$$\begin{aligned}
H_{\text{int},I} &= H_{\text{cl},I} + H_{\text{qu},I}, \sigma_{e_{\uparrow},I,i} \quad (\text{B1}) \\
H_{\text{cl},I} &= \Omega_{\text{probe}} \sum_{i=1}^N e^{i\mathbf{k}L\mathbf{r}_i} (|e_{\uparrow}\rangle_{I,i}\langle\downarrow| + |e_{\downarrow}\rangle_{I,i}\langle\uparrow|) + H.C., \\
H_{\text{qu},I} &= \sum_{i=1}^N \sum_{\mathbf{k}} \sum_{\hat{\lambda}_{\mathbf{k}}=1}^2 g_{\mathbf{k}} e^{i\mathbf{k}\mathbf{r}_i} a_{\mathbf{k}} (|e_{\downarrow}\rangle_{I,i}\langle\downarrow| e^{i\Omega t} + |e_{\uparrow}\rangle_{I,i}\langle\uparrow| e^{-i\Omega t} \\
&\quad + |\downarrow\rangle_{I,i}\langle e_{\downarrow}| e^{-i\Omega t} e^{-2i\omega_L t} + |\uparrow\rangle_{I,i}\langle e_{\uparrow}| e^{i\Omega t} e^{-2i\omega_L t}) + H.C., \\
&\quad + \sum_{i=1}^N \sum_{\mathbf{k}} \sum_{\hat{\lambda}_{\mathbf{k}}=1}^2 \check{g}_{\mathbf{k}} e^{i\mathbf{k}\mathbf{r}_i} a_{\mathbf{k}} (|e_{\uparrow}\rangle_{I,i}\langle\downarrow| + |e_{\downarrow}\rangle_{I,i}\langle\uparrow| \\
&\quad + |\downarrow\rangle_{I,i}\langle e_{\uparrow}| e^{-2i\omega_L t} + |\uparrow\rangle_{I,i}\langle e_{\downarrow}| e^{-2i\omega_L t}) + H.C.,
\end{aligned}$$

where $\hat{\lambda}_{\mathbf{k}}$ specifies the two orthogonal polarizations of the light mode with wave vector \mathbf{k} . $g_{\mathbf{k}} = \hat{\mathbf{e}}_{\mathbf{k}} \cdot \mathbf{p} \sqrt{\frac{\omega_{\mathbf{k}}}{2\epsilon_0 V}}$ is the coupling strength of desired transitions involving the quantum field, while $\check{g}_{\mathbf{k}}$ is the coupling strength corresponding to undesired transitions. $\hat{\mathbf{e}}_{\mathbf{k}}$ is the unit polarization vector, V is the quantization volume of the electromagnetic field, ϵ_0 the vacuum permittivity and \mathbf{p} is the transition matrix element of transitions $|e_{\uparrow}\rangle \rightarrow |\downarrow\rangle$ and $|e_{\downarrow}\rangle \rightarrow |\uparrow\rangle$. $H_{\text{int}} = H_{\text{int},I} + H_{\text{int},II}$. $H_{\text{int},II}$ is given by an expression analogous to Eq. (B1), where subscripts are changed accordingly ($I \rightarrow II$).

Based on this Hamiltonian, we derive a master equation for the reduced atomic density matrix $\rho(t)$ using the approximation of independent rates of variation and assuming Born-Markov dynamics as explained in Sec. III B

$$d_t \rho(t) = -i[H_{\text{cl}}, \rho(t)] + \mathcal{L}_{\text{qu}} \rho(t),$$

where \mathcal{L} is a Lindblad operator corresponding to the quantum part of the interaction H_{qu} . This master equation consists of three parts

$$d_t \rho(t) = L(\rho(t))_{\text{ens},I} + L(\rho(t))_{\text{ens},II} + L(\rho(t))_{\text{inter-ens.}}. \quad (\text{B2})$$

The first and second term $L(\rho(t))_{\text{ens},I}$ and $L(\rho(t))_{\text{ens},II}$ include only terms referring to the first and second ensemble respectively, while the third term $L(\rho(t))_{\text{inter-ens.}}$ summarizes all terms combining operators acting on both samples. The first term is given by

$$\begin{aligned}
L(\rho(t))_{\text{ens},I} &= -i[H_{\text{cl},I}, \rho(t)] \quad (\text{B3}) \\
&\quad + \frac{1}{2} \sum_{i,j} \mathcal{J}_{ij}^{I,I} |\uparrow\rangle_{I,i}\langle e_{\uparrow}| \rho(t) |e_{\uparrow}\rangle_{I,j}\langle\uparrow| \\
&\quad + \frac{1}{2} \sum_{i,j} \check{\mathcal{J}}_{ij}^{I,I} |\downarrow\rangle_{I,i}\langle e_{\uparrow}| \rho(t) |e_{\uparrow}\rangle_{I,j}\langle\downarrow| \\
&\quad + \dots,
\end{aligned}$$

where we used the approximation $\omega_L \gg \Omega$, which is very well justified for optical frequencies, and neglected fast

oscillating terms which appear in the standard derivation [60], if photonic modes in the upper and lower sideband are not treated as independent baths [61]. $\mathcal{J}_{ij}^{I,I} = \mathcal{J}_{ji}^{I,I}$ is a complex decay rate associated with desired transitions, while $\check{\mathcal{J}}_{ij}^{I,I} = \check{\mathcal{J}}_{ji}^{I,I}$ is the rate of undesired transitions. For the simple model discussed in Sec. III, $\check{\mathcal{J}}_{ij}^{I,I} = 2\mathcal{J}_{ij}^{I,I}$. Imaginary single particle terms $\text{Im}(\mathcal{J}_{ii}^{I,I})$ (Lamb shifts) are absorbed in the detunings as explained in Sec. III B. The second term $L(\rho(t))_{\text{ens},II}$ is given by an analogous expression with changed subscripts $I \mapsto II$.

The last term in Eq. (B2) can be written as sum $L(\rho(t))_{\text{inter-ens.}} = L(\rho(t))_{\text{inter-ens.}}^{I,II} + L(\rho(t))_{\text{inter-ens.}}^{II,I}$. The first part is given by

$$\begin{aligned}
L(\rho(t))_{\text{inter-ens.}}^{I,II} &= \frac{1}{2} \sum_{i,j} \mathcal{J}_{ij}^{I,II} |\uparrow\rangle_{I,i}\langle e_{\uparrow}| \rho(t) |e_{\downarrow}\rangle_{II,j}\langle\downarrow| \\
&\quad + \frac{1}{2} \sum_{i,j} \mathcal{J}_{ij}^{I,II} |\downarrow\rangle_{I,i}\langle e_{\downarrow}| \rho(t) |e_{\uparrow}\rangle_{II,j}\langle\uparrow| \\
&\quad + \frac{1}{2} \sum_{i,j} \check{\mathcal{J}}_{ij}^{I,II} |\uparrow\rangle_{I,i}\langle e_{\downarrow}| \rho(t) |e_{\uparrow}\rangle_{II,j}\langle\downarrow| \\
&\quad + \frac{1}{2} \sum_{i,j} \check{\mathcal{J}}_{ij}^{I,II} |\downarrow\rangle_{I,i}\langle e_{\uparrow}| \rho(t) |e_{\downarrow}\rangle_{II,j}\langle\uparrow| \\
&\quad + \dots \quad (\text{B4})
\end{aligned}$$

and $L(\rho(t))_{\text{inter-ens.}}^{II,I}$ is given by an analogous expression with changed subscripts ($I \rightarrow II$). Decay rates appearing in inter-ensemble terms differ from single-ensemble rates $\mathcal{J}_{ij}^{I,I} = \mathcal{J}_{ij}^{II,II}$

$$\mathcal{J}_{ij}^{I,II} = e^{-i\mathbf{k}\mathbf{R}} \mathcal{J}_{ij}^{I,I}, \quad \mathcal{J}_{ij}^{II,I} = e^{+i\mathbf{k}\mathbf{R}} \mathcal{J}_{ij}^{I,I}$$

where \mathbf{R} is the distance between the two ensembles. In order to obtain compact expressions, we use the simplified notation \mathcal{J}_{ij} for single ensemble or inter-ensemble rates depending to which samples the indices i and j refer. We use the convention $\mathbf{r}_{ij} = \mathbf{r}_i - \mathbf{r}_j - \mathbf{R}$ if the atom with index j is located in the second ensemble. (However, in App. B2, it is shown that the distance between the ensembles does not play a role in the setting considered here.) Using this notation, \mathcal{J}_{ij} is given by

$$\mathcal{J}_{ij} = \int d\mathbf{k} \sum_{\hat{\lambda}_{\mathbf{k}}=1}^2 \check{g}^2(\mathbf{k}) e^{i\mathbf{k}(\mathbf{r}_i - \mathbf{r}_j)} \int_0^{\infty} d\tau (e^{-i(\omega_{\mathbf{k}} - \omega_L)\tau} + e^{-i(\omega_{\mathbf{k}} + \omega_L)\tau}),$$

where the sum over light modes was changed into an integral $\sum_{\mathbf{k}} \rightarrow \frac{V}{(2\pi)^3} \int d\mathbf{k}$. The prefactor is absorbed in the coupling constant $g(\mathbf{k}) = \sqrt{V/(2\pi)^3} g_{\mathbf{k}}$ whenever an integral over light modes is used. The second term in the expression in brackets ($e^{-i(\omega_{\mathbf{k}} + \omega_L)\tau}$) stems from counter-rotating terms in the Hamiltonian, and would not appear if the rotating wave approximation had been applied. Using the identity $\int_0^{\infty} e^{i\omega\tau} = \pi\delta(\omega) + i\mathcal{P}(1/\omega)$,

where \mathcal{P} is the principal value, we obtain

$$\begin{aligned} \text{Re}(\mathcal{J}_{ij}) &= \pi \int d\mathbf{k} \sum_{\hat{\lambda}_k=1}^2 g^2(\mathbf{k}) e^{i\mathbf{k}(\mathbf{r}_i - \mathbf{r}_j)} \delta(\omega_k - \omega_L), \\ \text{Im}(\mathcal{J}_{ij}) &= i\mathcal{P} \left(\int d\mathbf{k} \sum_{\hat{\lambda}_k=1}^2 g^2(\mathbf{k}) e^{i\mathbf{k}(\mathbf{r}_i - \mathbf{r}_j)} \left(\frac{1}{\omega_L - \omega_k} + \frac{1}{\omega_L + \omega_k} \right) \right), \end{aligned}$$

These rates can be calculated as shown in [62] (compare Eqs. (9) and (10)).

Now, a master equation for the reduced density matrix of atomic ground states $\mathbb{P}_g \rho(t) \mathbb{P}_g$ is derived by applying the projector $\mathbb{P}_g = \bigotimes_{i,j=1}^N (|\uparrow\rangle_{I,i} \langle\uparrow| + |\downarrow\rangle_{I,i} \langle\downarrow|) \otimes (|\uparrow\rangle_{II,j} \langle\uparrow| + |\downarrow\rangle_{II,j} \langle\downarrow|)$ to the differential equation $d_t \rho(t) = L(\rho(t))_{\text{ens.I}} + L(\rho(t))_{\text{ens.II}} + L(\rho(t))_{\text{inter-ens.}}$ using Eqs. (B3) and (B4). Excited states are eliminated under the condition $\Delta_{\uparrow,I/II}, \Delta_{\downarrow,I/II} \gg \Gamma_{\text{atomic}}$, using $d_t \mathbb{P}_e \rho(t) \mathbb{P}_g = d_t \mathbb{P}_g \rho(t) \mathbb{P}_e = d_t \mathbb{P}_e \rho(t) \mathbb{P}_e = 0$, where $\mathbb{P}_e = \mathbb{I} - \mathbb{P}_g$. Moreover, we assume that terms corresponding to states with two or more excitations, for example terms of the type $\mathbb{P}_e^{(2)} \rho(t) \mathbb{P}_g$, are negligible compared to terms corresponding to states where at most one atom is in an excited state like $\mathbb{P}_e^{(1)} \rho(t) \mathbb{P}_g$. $\mathbb{P}_e^{(1)} = \sum_{i=1}^N \mathbb{P}_{e,I,i} \otimes \mathbb{P}_{g,II} + \sum_{j=1}^N \mathbb{P}_{g,I} \otimes \mathbb{P}_{e,II,j}$ with $\mathbb{P}_{e,i,I/II} = \bigotimes_{i=1}^N (|e_{\uparrow}\rangle_{I/II,i} \langle e_{\uparrow}| + |e_{\downarrow}\rangle_{I/II,i} \langle e_{\downarrow}|)$. $\mathbb{P}_e^{(2)}$ is defined analogously. In the following we denote the resulting reduced density matrix of atomic ground states $\mathbb{P}_g \rho(t) \mathbb{P}_g$ simply by $\rho(t)$. We obtain

$$\begin{aligned} d_t \rho(t) &= \frac{\Omega_{\text{probe}}}{2} \sum_{i,j} e^{-i\mathbf{k}_L(\mathbf{r}_j - \mathbf{r}_i)} (\\ &\mathcal{J}_{ij} \left(\frac{\sigma_{I,i}}{\Delta_{\uparrow,I}} + \frac{\sigma_{II,j}^{\dagger}}{\Delta_{\downarrow,II}} \right) \rho(t) \left(\frac{\sigma_{I,i}^{\dagger}}{\Delta_{\uparrow,I}} + \frac{\sigma_{II,j}}{\Delta_{\downarrow,II}} \right) \\ &+ \mathcal{J}_{ij} \left(\frac{\sigma_{II,i}}{\Delta_{\uparrow,II}} + \frac{\sigma_{I,j}^{\dagger}}{\Delta_{\downarrow,I}} \right) \rho(t) \left(\frac{\sigma_{II,i}^{\dagger}}{\Delta_{\uparrow,II}} + \frac{\sigma_{I,j}}{\Delta_{\downarrow,I}} \right) \\ &+ \check{\mathcal{J}}_{ij} \left(\frac{\sigma_{\downarrow\downarrow,I,i}}{\Delta_{\uparrow,I}} + \frac{\sigma_{\uparrow\uparrow,II,j}^{\dagger}}{\Delta_{\downarrow,II}} \right) \rho(t) \left(\frac{\sigma_{\downarrow\downarrow,I,i}}{\Delta_{\uparrow,I}} + \frac{\sigma_{\uparrow\uparrow,II,j}^{\dagger}}{\Delta_{\downarrow,II}} \right) \\ &+ \check{\mathcal{J}}_{ij} \left(\frac{\sigma_{\downarrow\downarrow,II,i}}{\Delta_{\uparrow,II}} + \frac{\sigma_{\uparrow\uparrow,I,j}^{\dagger}}{\Delta_{\downarrow,I}} \right) \rho(t) \left(\frac{\sigma_{\downarrow\downarrow,II,i}}{\Delta_{\uparrow,II}} + \frac{\sigma_{\uparrow\uparrow,I,j}^{\dagger}}{\Delta_{\downarrow,I}} \right) \\ &+ \dots, \end{aligned}$$

where the abbreviations $\sigma_{\uparrow\uparrow,I/II,i} = |\uparrow\rangle_{I/II,i} \langle\uparrow|$ and $\sigma_{\downarrow\downarrow,I/II,i} = |\downarrow\rangle_{I/II,i} \langle\downarrow|$ were used. Terms with prefactors $1/\Delta^3$ have been neglected since we assume that detunings are large. AC-Stark shifts

$$\begin{aligned} d_t \rho(t)|_{\text{AC Stark}} &= -i\Omega_{\text{probe}} \sum_{i=1}^N \left[\frac{\sigma_{\uparrow\uparrow,I,i}}{\Delta_{\downarrow,I}} + \frac{\sigma_{\downarrow\downarrow,I,i}}{\Delta_{\uparrow,I}}, \rho(t) \right] \\ &+ i\Omega_{\text{probe}} \sum_{i=1}^N \left[\frac{\sigma_{\uparrow\uparrow,II,i}}{\Delta_{\downarrow,I}} + \frac{\sigma_{\downarrow\downarrow,II,i}}{\Delta_{\uparrow,I}}, \rho(t) \right] \end{aligned}$$

are absorbed in the detunings. Using the definitions $\mu_{I/II} = \pm \frac{\Delta + \Omega}{2\sqrt{\Delta\Omega}}$, $\nu_{I/II} = \pm \frac{\Delta - \Omega}{2\sqrt{\Delta\Omega}}$ [57] and $J_{ij} = \mathcal{J}_{ij} 2\Omega_{\text{probe}} \sqrt{\Delta\Omega} / (\Delta^2 - \Omega^2)$, one obtains

$$\begin{aligned} d_t \rho(t) &= \frac{1}{2} \sum_{i,j=1}^N e^{-i\mathbf{k}_L(\mathbf{r}_j - \mathbf{r}_i)} J_{ij} \left(A_i \rho(t) A_j^{\dagger} + B_i \rho(t) B_j^{\dagger} \right) \\ &+ \frac{1}{2} \sum_{i,j=1}^N e^{-i\mathbf{k}_L(\mathbf{r}_j - \mathbf{r}_i)} \check{J}_{ij} \left(C_i \rho(t) C_j^{\dagger} + D_i \rho(t) D_j^{\dagger} \right) \\ &+ \dots \end{aligned} \quad (\text{B5})$$

with

$$\begin{aligned} A_i &= \mu_I \sigma_{I,i} + \nu_{II} \sigma_{I,i}^{\dagger}, \\ B_i &= \mu_{II} \sigma_{II,i} + \nu_I \sigma_{I,i}^{\dagger}, \\ C_i &= \mu_I \sigma_{\downarrow\downarrow,I,i} + \nu_{II} \sigma_{\uparrow\uparrow,II,i}, \\ D_i &= \mu_{II} \sigma_{\downarrow\downarrow,II,i} + \nu_I \sigma_{\uparrow\uparrow,I,i}. \end{aligned}$$

The expressions in the main text are obtained by introducing a unified notation (compare Eq. (8)), which absorbs the relative sign μ_I/μ_{II} in atomic operators referring to the second ensemble $\sigma_{II} \rightarrow \text{sgn}(\mu_I \mu_{II}) \sigma_{II}$.

2. Master equation including atomic motion

Below, we include thermal motion of particles, by treating atomic positions as classical random variables. We start from the master equation for atomic ground states (B5). As outlined in Sec. III C, random atomic positions can be taken into account by introducing averaged coefficients in the master equation. Averaged rates $\langle J_{ij} \rangle$ are calculated assuming Gaussian distributions with width L for atomic positions in the two ensembles. We start by calculating the rate corresponding to moving particles in a single ensemble. Below it is shown that for inter-ensemble rates the same result is obtained for the setup and range of parameters considered here.

$$\begin{aligned} \langle J_{ij} \rangle &= \frac{1}{\pi^3 L^6} \int d\mathbf{r} \int d\hat{\mathbf{r}} e^{i\mathbf{k}_L(\mathbf{r} - \hat{\mathbf{r}}) - \frac{r^2 + \hat{r}^2}{L^2}} (\gamma(\mathbf{r} - \hat{\mathbf{r}}) + ig(\mathbf{r} - \hat{\mathbf{r}})), \\ &= \frac{1}{(2\pi)^{3/2} L^3} \int d\mathbf{r} e^{i\mathbf{k}_L \mathbf{r} - \frac{r^2}{2L^2}} (\gamma(\mathbf{r}_-) + ig(\mathbf{r}_-)), \end{aligned} \quad (\text{B6})$$

where the variable transformation $\mathbf{r}_+ = \mathbf{r} + \hat{\mathbf{r}}$, $\mathbf{r}_- = \mathbf{r} - \hat{\mathbf{r}}$ was made in the second step. The single particle rate is given by $J_{ii} = \Gamma$ (Lamb shifts are absorbed in the detunings). Now, averaged rates $\langle J_{ij} \rangle$ with $i \neq j$ need to be determined. We consider now first the real part and then the imaginary part of the averaged decay rate $\langle J_{ij} \rangle$.

The real part $\Gamma_{ij} = \text{Re}(\langle J_{ij} \rangle)$ is calculated by inserting Eq. (9) into Eq. (B6) and fixing $\hat{\mathbf{p}} = \hat{\mathbf{x}}$ and $\hat{\mathbf{k}}_L = \hat{\mathbf{z}}$. $\Gamma_{ij} = \Gamma_{ij,A} + \Gamma_{ij,B}$ is a sum of two contributions

corresponding to the first and the second line in Eq. (9). The first term is given by

$$\Gamma_{ij,A} = \frac{3\Gamma}{\sqrt{2\pi}L^3} \int_0^\infty dr_- r_-^2 e^{-\frac{r_-^2}{2L^2}} \frac{\sin(k_L r_-)}{k_L r_-} \left(\frac{\sin(k_L r_-)}{k_L r_-} + \frac{\cos(k_L r_-)}{(k_L r_-)^2} - \frac{\sin(k_L r_-)}{(k_L r_-)^3} \right). \quad (\text{B7})$$

The integrand of this expression tends to zero in the limit $r_- \rightarrow 0$. This can for example be seen by expanding the integrand for small values $r_- \ll 1$, $r_-^2 e^{-\frac{r_-^2}{2L^2}} \frac{\sin(k_L r_-)}{k_L r_-} \left(\frac{\sin(k_L r_-)}{k_L r_-} + \frac{\cos(k_L r_-)}{(k_L r_-)^2} - \frac{\sin(k_L r_-)}{(k_L r_-)^3} \right) = \frac{2}{3} r_-^2 + \mathcal{O}(r_-^4)$. Hence the dominant contribution in the limit $k_L L \gg 1$, stems from the first term in brackets $\sin(k_L r_-)/(k_L r_-)$. The other two terms in brackets decay faster in the interatomic distance r_- and lead only to corrections on the order of $1/(k_L L)^4$. For $k_L L \gg 1$,

$$\begin{aligned} \Gamma_{ij,A} &= \frac{3\Gamma}{\sqrt{2\pi}L^3} \int_0^\infty dr_- r_-^2 e^{-\frac{r_-^2}{2L^2}} \frac{\sin(k_L r_-)^2}{(k_L r_-)^2} \\ &= \frac{3}{4} \Gamma \frac{1}{(k_L L)^2} (1 - e^{-2k_L L}), \end{aligned}$$

which can be approximated by $\Gamma_{ij,A} = \frac{3}{4} \Gamma \frac{1}{(k_L L)^2}$. The second part

$$\begin{aligned} \Gamma_{ij,B} &= \frac{3\Gamma}{\sqrt{2\pi}L^3} \int_0^\infty dr_- r_-^2 e^{-\frac{r_-^2}{2L^2}} \left(\frac{\cos(k_L r_-)}{(k_L r_-)^2} - \frac{\sin(k_L r_-)}{(k_L r_-)^3} \right) \\ &\quad \left(\frac{\sin(k_L r_-)}{k_L r_-} + \frac{3 \cos(k_L r_-)}{(k_L r_-)^2} - \frac{3 \sin(k_L r_-)}{(k_L r_-)^3} \right), \end{aligned}$$

is negligible compared to the first part $\Gamma_{ij,A}$ in the asymptotic limit $k_L L \rightarrow \infty$. Its integrand tends to zero for $r_- \rightarrow 0$ (expansion for $r_- \ll 1$ yields $k_L^2 r_-^4/45 + \mathcal{O}(r_-^5)$) and contains only terms proportional to $\cos(k_L r_-) \sin(k_L r_-)/(k_L r_-)^x$, $\cos(k_L r_-)^2/(k_L r_-)^x$ and $\sin(k_L r_-)^2/(k_L r_-)^x$ with $x \geq 1$. These types of terms have been neglected in Eq. (B7) or decay even faster in r_- . Since $\Gamma_{ij,B}$ is negligible compared to $\Gamma_{ij,A}$, we use $\Gamma_{ij} = \Gamma \frac{3}{4(k_L L)^2}$.

Next, we calculate the imaginary part $G_{ij} = \text{Im}(\langle J_{ij} \rangle)$ by inserting Eq. (10) into Eq. (B6). As before, we consider the two contributions $G_{ij} = G_{ij,A} + G_{ij,B}$ corresponding to the first and the second line in Eq. (10) separately. The integrand of the first part

$$\begin{aligned} G_{ij,A} &= -\frac{3\Gamma}{\sqrt{2\pi}L^3} \int_0^\infty dr_- r_-^2 e^{-\frac{r_-^2}{2L^2}} \frac{\cos(k_L r_-)}{k_L r_-} \\ &\quad \left(\frac{\sin(k_L r_-)}{k_L r_-} + \frac{\cos(k_L r_-)}{(k_L r_-)^2} - \frac{\sin(k_L r_-)}{(k_L r_-)^3} \right), \end{aligned}$$

tends to zero for $r_- \rightarrow 0$ (expansion for $r_- \ll 1$ yields $2r_-/(3k_L) + \mathcal{O}(r_-^3)$) and features a rapidly

oscillating term proportional to $\sin(k_L r_-) \cos(k_L r_-)$ in the integral, which leads to a contribution which scales with $1/(k_L L)^3$. The other terms proportional to $\cos^2(k_L L)/(k_L L)^3$ and $\cos(k_L L) \sin(k_L L)/(k_L L)^3$ are again of the type discussed and neglected before. Hence it is well justified to assume that $G_{ij,I} \ll \Gamma_{ij,I}$. The integrand of the second part

$$\begin{aligned} G_{ij,B} &= \frac{3\Gamma}{\sqrt{2\pi}L^3} \int_0^\infty dr_- r_-^2 e^{-\frac{r_-^2}{2L^2}} \left(\frac{\sin(k_L r_-)}{(k_L r_-)^2} + \frac{\cos(k_L r_-)}{(k_L r_-)^3} \right) \\ &\quad \left(\frac{\sin(k_L r_-)}{k_L r_-} + \frac{3 \cos(k_L r_-)}{(k_L r_-)^2} - \frac{3 \sin(k_L r_-)}{(k_L r_-)^3} \right), \end{aligned}$$

also tends to zero for $r_- \rightarrow 0$ (expansion for $r_- \ll 1$ yields $-r_-/(15k_L) + \mathcal{O}(r_-^3)$) and contains only one term which has not been considered so far. The term in the integrand proportional $\sin(k_L r_-)^2/(k_L r_-)$ leads to a contribution which decays with $\log(k_L L)/(k_L L)^3$ in the asymptotic limit $k_L L \rightarrow \infty$. The imaginary part of the averaged decay rate $\langle J_{ij} \rangle$ is therefore negligible compared to the real part.

The distance between the two atomic samples does not play a role in the setting under consideration. In the limit $k_L \gg R/L^2$, averaged single ensemble rates equal averaged inter-ensemble rates $\langle J_{ij} \rangle = \langle J_{ij} \rangle^{I,I} = \langle J_{ij} \rangle^{I,II}$. In the following, we outline the calculation of the inter-ensemble value $\Gamma_{ij,A}^{I,II}$. Analogous arguments can be used to compute $\Gamma_{ij,B}^{I,II}$, $G_{ij,A}^{I,II}$, and $G_{ij,B}^{I,II}$.

Inter-ensemble rates are obtained by averaging atomic positions with respect to Gaussian distributions centered at the origin and a distance R apart respectively

$$\begin{aligned} \Gamma_{ij}^{I,II} &= \frac{1}{\pi^3 L^6} \int d\mathbf{r} \int d\mathbf{r}' e^{i\mathbf{k}_L(\mathbf{r}-\mathbf{r}')} e^{-\frac{r_-^2}{L^2}} e^{-\frac{(\mathbf{r}-\mathbf{R})^2}{L^2}} \gamma(\mathbf{r}-\mathbf{r}'), \\ &= \frac{1}{(2\pi)^3 L^6} \int d\mathbf{r}_+ \int d\mathbf{r}_- e^{i\mathbf{k}_L \mathbf{r}_-} e^{-\frac{(\mathbf{r}_-+\mathbf{R})^2}{2L^2}} e^{-\frac{(\mathbf{r}_+-\mathbf{R})^2}{2L^2}} \gamma(\mathbf{r}_-), \\ &= \frac{1}{(2\pi)^{3/2} L^3} \int d\mathbf{r}_- e^{i\mathbf{k}_L \mathbf{r}_-} e^{-\frac{(\mathbf{r}_-+\mathbf{R})^2}{2L^2}} \gamma(\mathbf{r}_-), \end{aligned}$$

where the variable transformation $\mathbf{r}_+ = \mathbf{r} + \mathbf{r}'$, $\mathbf{r}_- = \mathbf{r} - \mathbf{r}'$ was made, as before. By inserting Eq. (9) and neglecting the dipole factor $(\hat{\mathbf{x}} \cdot (\mathbf{r} - \mathbf{r}')/|\mathbf{r} - \mathbf{r}'|)^2$, which does not play a role for the distance under consideration [74], one obtains

$$\begin{aligned} \Gamma_{ij}^{I,II} &= \frac{3\Gamma}{2(2\pi)^{3/2} L^3} \int d\mathbf{r}_- e^{i\mathbf{k}_L \mathbf{r}_-} e^{-\frac{(\mathbf{r}_-+\mathbf{R})^2}{2L^2}} \frac{\sin(k_L r_-)}{k_L r_-}, \\ &= \frac{3\Gamma}{2\sqrt{2\pi}L^3} \int_0^\infty dr_- r_-^2 \frac{\sin(k_L r_-)}{k_L r_-} \int_0^\pi d\theta \sin(\theta) \\ &\quad e^{ik_L r_- \cos(\theta)} e^{-\frac{1}{2L^2}(r_-^2 + R^2 + 2r_- R \cos(\theta))}, \\ &= \frac{3\Gamma}{2\sqrt{2\pi}L^3 k_L} \int_0^\infty dr_- \sin(k_L r_-) e^{-\frac{(r_-^2 + R^2)}{2L^2}} \\ &\quad \int_{-r_-}^{r_-} dx e^{-ik_L x} e^{\frac{Rx}{L^2}}. \end{aligned}$$

In the last step, the integral over θ was transformed using the variable transformation $x = -\cos(\theta)r_-$. The integral over x can be directly evaluated yielding

$$\begin{aligned}\Gamma_{ij}^{I,II} &= \frac{3\Gamma}{2\sqrt{2\pi}L^3k_L(ik_L - R/L^2)} \int_0^\infty dr_- \sin(k_L r_-) \\ &\quad e^{-\frac{(r_-+R)^2}{2L^2}} \left(e^{ik_L r_- - \frac{Rr_-}{L^2}} - e^{-ik_L r_- + \frac{Rr_-}{L^2}} \right), \\ &= \frac{3\Gamma}{2\sqrt{2\pi}L^3k_L(ik_L - R/L^2)} \int_{-\infty}^\infty dr_- \sin(k_L r_-) \\ &\quad e^{-\frac{(r_-+R)^2}{2L^2}} e^{ik_L r_-}.\end{aligned}$$

As next step, the variable transformation $\tilde{r} = r_- + R$ is made such that

$$\begin{aligned}\Gamma_{ij}^{I,II} &= \frac{3\Gamma}{2\sqrt{2\pi}L^3k_L(ik_L - R/L^2)} \int_{-\infty}^\infty d\tilde{r} \sin(k_L(\tilde{r} - R)), \\ &\quad e^{-\frac{\tilde{r}^2}{2L^2}} e^{ik_L(\tilde{r}-R)} \\ &= \frac{3\Gamma}{4\sqrt{2\pi}L^3k_L(-k_L - iR/L^2)} \int_{-\infty}^\infty d\tilde{r} e^{-\frac{\tilde{r}^2}{2L^2}}, \\ &\quad (e^{2ik_L(\tilde{r}-R)} - 1), \\ &= \frac{3\Gamma}{4(L^2k_L^2 + ik_LR)} \left(1 - e^{-2k_L^2L^2 - 2ik_LR} \right)\end{aligned}$$

which yields $\Gamma_{ij}^{I,II} = \Gamma \frac{3}{4(k_L L)^2}$ for $k_L \gg R/L^2$ and $k_L L \gg 1$.

Appendix C: Time evolution of entanglement in a two-level model

In this appendix, we calculate the amount of entanglement produced $\xi(t)$ (compare Eq. (3)) for the model described in Sec. III. The first part of this appendix C1 covers the derivation of $\xi(t)$ based on the full master equation (13). The second part C2 contains explanations concerning Eq. (13).

1. Time evolution of entanglement

In the following, the time evolution of entanglement $\xi(t)$ is calculated. To this end we calculate the single-ensemble variance of transverse spin components $\text{var}(J_z) = \langle J_z^2 \rangle - \langle J_z \rangle^2$, the inter-ensemble product of transverse spins $\langle J_{z,I} J_{z,II} \rangle$ and finally the mean value of the longitudinal spin $\langle J_x \rangle$.

We start by calculating $d_t \langle J_z^2 \rangle_t$. The dissipative evolution described by Eq. (13) leads to

$$d_t \langle J_z^2 \rangle = -\tilde{\Gamma} \langle J_z^2 \rangle - \frac{2d}{N} \Gamma \langle J_z^2 J_x \rangle + \frac{N}{4} \tilde{\Gamma} + \frac{d\Gamma}{N} \langle J_x^2 \rangle (\mu^2 + \nu^2).$$

Applying the decorrelation approximation $\langle J_z J_x \rangle \approx \langle J_z \rangle \langle J_x \rangle$ [75] for mean values of products of transverse

and longitudinal spin yields

$$d_t \langle J_z^2 \rangle = -\left(\tilde{\Gamma} + d\Gamma P_2(t) \right) \langle J_z^2 \rangle + \frac{N}{4} \left(\tilde{\Gamma} + d\Gamma P_2(t) \right)^2 (\mu^2 + \nu^2)$$

and similarly

$$d_t \langle J_y^2 \rangle = -\left(\tilde{\Gamma} + d\Gamma P_2(t) \right) \langle J_y^2 \rangle + \frac{N}{4} \left(\tilde{\Gamma} + d\Gamma P_2(t) \right)^2 (\mu^2 + \nu^2)$$

where $\langle J_x \rangle = \frac{N}{2} P_2(t)$ and $\langle J_x^2 \rangle \approx \langle J_x \rangle^2 = \frac{N^2}{4} P_2(t)^2$ were used. The latter approximation leads only to an error of the order $\mathcal{O}(\frac{1}{N})$ [76] Next, the mean values of the transverse spin components are computed using the same approximations.

$$d_t \langle J_{y/z} \rangle_t = -\frac{1}{2} \left(\tilde{\Gamma} + d\Gamma P_2(t) \right) \langle J_{y/z} \rangle_t,$$

with $\langle J_{y/z} \rangle_{t=0} = 0$. The mean values can therefore be ignored when calculating single ensemble variances $\text{var}(J_{y/z})$.

The time derivatives of inter-ensemble products of transverse spins are given by

$$d_t \langle J_{z,I} J_{z,II} \rangle = -\left(\tilde{\Gamma} + d\Gamma P_2(t) \right) \langle J_{z,I} J_{z,II} \rangle + \frac{N}{2} \mu \nu d\Gamma P_2(t)^2,$$

$$d_t \langle J_{y,I} J_{y,II} \rangle = -\left(\tilde{\Gamma} + d\Gamma P_2(t) \right) \langle J_{y,I} J_{y,II} \rangle - \frac{N}{2} \mu \nu d\Gamma P_2(t)^2,$$

where we used $\langle J_{x,I} J_{x,II} \rangle \approx \langle J_{x,I} \rangle \langle J_{x,II} \rangle$. For $N \gg 1$, this is a very good approximation, since collective effects on populations are suppressed by a factor d/N . Therefore, the time evolution of longitudinal spins is only determined by single-particle terms, which do not lead to correlations between the two ensembles. Hence, the variances of the non-local operators $J_{y,\pm} = (J_{y,I} \pm J_{y,II})/\sqrt{2}$ and $J_{z,\pm} = (J_{z,I} \pm J_{z,II})/\sqrt{2}$ evolve according to

$$\begin{aligned}d_t \text{var}(J_{y,\pm}) &= -\left(\tilde{\Gamma} + d\Gamma P_2(t) \right) \text{var}(J_{y,\pm}) \quad (\text{C1}) \\ &\quad + \frac{N}{4} \left(\tilde{\Gamma} + d\Gamma P_2(t) \right)^2 (\mu \mp \nu)^2,\end{aligned}$$

$$\begin{aligned}d_t \text{var}(J_{z,\pm}) &= -\left(\tilde{\Gamma} + d\Gamma P_2(t) \right) \text{var}(J_{z,\pm}) \quad (\text{C2}) \\ &\quad + \frac{N}{4} \left(\tilde{\Gamma} + d\Gamma P_2(t) \right)^2 (\mu \pm \nu)^2,\end{aligned}$$

such that

$$\text{var}(J_{y,\pm})_\infty = \text{var}(J_{z,\mp})_\infty = \frac{N}{4} \frac{\tilde{\Gamma} + d\Gamma P_{2,\infty}^2 (\mu \mp \nu)^2}{\tilde{\Gamma} + d\Gamma P_{2,\infty}}$$

in the steady state. The variances $\text{var}(J_{y,+})$ and $\text{var}(J_{z,-})$ are squeezed, while $\text{var}(J_{y,-})$ and $\text{var}(J_{z,+})$ are anti-squeezed. Now, we consider the time evolution of the longitudinal spin

$$d_t |\langle J_x \rangle| = -\frac{N}{2} (\Gamma_{\text{heat}} - \Gamma_{\text{cool}}) - (\Gamma_{\text{heat}} + \Gamma_{\text{cool}}) |\langle J_x \rangle|,$$

which yields directly

$$|\langle J_x \rangle|_\infty = \frac{N}{2} \frac{\Gamma_{\text{cool}} - \Gamma_{\text{heat}}}{\Gamma_{\text{cool}} + \Gamma_{\text{heat}}} = \frac{N}{2} P_{2,\infty}$$

for $t \rightarrow \infty$.

Collective effects have an negligible effect on the time evolution of the polarization. $P_2(t)$ evolves due to single-particle effects only and hence much slower than $\text{var}(J_{y,\pm})$ and $\text{var}(J_{z,\pm})$ for samples with high optical depth. In this case, the solution for $\xi(t) = \text{var}(J_{z,+})/P_2(t)$ can be cast in a simple analytical form

$$\xi(t) = \frac{1}{P_2(t)} e^{-(\tilde{\Gamma} + d\Gamma P_2(t))t} + \frac{1}{P_2(t)} \frac{\tilde{\Gamma} + d\Gamma P_2(t)^2 (|\mu| - |\nu|)^2}{\tilde{\Gamma} + d\Gamma P_2(t)} \left(1 - e^{-(\tilde{\Gamma} + d\Gamma P_2(t))t}\right).$$

2. Full master equation

In the following, we comment on the form of Eq. (13), in particular on the absence of collective noise terms.

The probe fields considered in Sec. III are off-resonant and it has been shown in the main text that collective contributions feature an enhancement factor which renders them the dominant decay mechanism for samples with high optical depth. As is shown in Sec. III D, it can be advantageous to apply also resonant laser light (pump fields). In contrast to off-resonant fields, collective contributions are negligible compared to single-particle terms for resonant light in the situation considered here. Unlike off-resonant collective rates, resonant collective rates are much slower than the corresponding single-particle rates for samples with high optical depth, which is an effect well known and harnessed in electromagnetically induced transparency [77–80]. The single particle decay rate after adiabatic elimination of excited states is given by $\Gamma_{\text{res}} = \frac{\Omega_{\text{pump}}^2}{\gamma_{\text{LW}}}$, where Ω_{pump} is the Rabi frequency of the applied laser field and γ_{LW} is the natural line width of excited levels. Coherent effective effects lead to an enhancement factor d in the denominator. Intuitively, this effect can be understood by noting that emitted resonant photons are reabsorbed in an optically thick medium.

Due to atomic motion in ensembles at room temperature, spectral lines are Doppler broadened. We take therefore off-resonant contributions of pump fields to the master equation with a detuning on the order of the Doppler width δ_{Doppler} into account. A calculation along the lines of the derivation shown in Sec. C 1 shows that these terms are negligible compared to their single-atom counterparts. More specifically, collective terms corresponding to a detuning δ_{Doppler} lead to decay

rates proportional to $\frac{\Omega_{\text{pump}}^2}{\delta_{\text{Doppler}}} \gamma_{\text{LW}} d = \frac{\Omega_{\text{pump}}^2}{\gamma_{\text{LW}} d} \left(\frac{\gamma_{\text{LW}} d}{\delta_{\text{Doppler}}}\right)^2$ with $|\delta_{\text{Doppler}}| \gg \gamma_{\text{LW}} d$, while single particle resonant terms lead to decay rates proportional to $\frac{\Omega_{\text{pump}}^2}{\gamma_{\text{LW}}}$.

Finally, Eq. (13) does not include collective terms, corresponding to radiative processes which do not change the internal atomic state, since they do not have an effect on the amount of entanglement generated. A master equation corresponding to the terms omitted in Eq. (12)

$$d_t \rho(t) = d \frac{\tilde{\Gamma}}{2} C \rho(t) C^\dagger + d \frac{\tilde{\Gamma}}{2} D \rho(t) D^\dagger + \dots,$$

with operators $C = \sum_i (\mu \sigma_{\downarrow\downarrow,II,i} + \nu \sigma_{\uparrow\uparrow,II,i})$ and $D = C = \sum_i (\mu \sigma_{\downarrow\downarrow,II,i} + \nu \sigma_{\uparrow\uparrow,II,i})$ leads to $d_t \xi(t) = 0$. Since $d_t \langle J_y \rangle = -\frac{d\tilde{\Gamma}}{2N} \langle J_y \rangle$, $d_t \langle J_z \rangle = -\frac{d\tilde{\Gamma}}{2N} \langle J_z \rangle$, and $d_t \langle J_x \rangle = 0$, $\langle J_y \rangle = \langle J_z \rangle = 0$ and $\langle J_z \rangle = N/2$ for all times. The time derivatives of single-ensemble variances for transverse spin components is given by

$$d_t \langle J_y^2 \rangle = \tilde{\Gamma} \frac{d}{N} (\mu^2 + \nu^2) (-\langle J_y^2 \rangle + \langle J_z^2 \rangle),$$

$$d_t \langle J_z^2 \rangle = \tilde{\Gamma} \frac{d}{N} (\mu^2 + \nu^2) (\langle J_y^2 \rangle - \langle J_z^2 \rangle),$$

such that $\langle J_y^2 \rangle = \langle J_z^2 \rangle = N/4$, for all times. Accordingly, $\langle J_{y,I} J_{y,II} \rangle = \langle J_{z,I} J_{z,II} \rangle = 0$ for all times since

$$d_t \langle J_{y,I} J_{y,II} \rangle = -2 \frac{d}{N} \hat{\Gamma} \mu \nu \langle J_{z,I} J_{z,II} \rangle,$$

$$d_t \langle J_{z,I} J_{z,II} \rangle = 2 \frac{d}{N} \hat{\Gamma} \mu \nu \langle J_{y,I} J_{y,II} \rangle.$$

The processes under consideration do not create entanglement unlike the terms in Eq. (12) with jump operators A and B . As shown above, they do not degrade entanglement either. Collective terms corresponding to far off-resonant radiative transitions $|\uparrow\rangle \rightarrow |e_\downarrow\rangle \rightarrow |\uparrow\rangle$, $|\downarrow\rangle \rightarrow |e_\uparrow\rangle \rightarrow |\downarrow\rangle$ do not introduce random phases and preserve coherence. The emitted photon does not reveal information about the internal atomic state, since it is emitted into the laser mode. Terms with jump operators C and D lead only to very small correction terms proportional to $1/N$ and can be ignored.

Appendix D: Generation of steady state entanglement in alkali atoms

In this appendix, we consider the generation of dissipatively driven entanglement in multi-level systems based on the model described in Sec. IV A.

Taking three ground state levels $|\uparrow\rangle$, $|\downarrow\rangle$ and $|h\rangle$ into account, as shown in Fig. 6, the evolution of the reduced atomic density matrix can be described by the

master equation

$$\begin{aligned}
d_t \rho(t) = & d\Gamma A \rho(t) A^\dagger + d\Gamma B \rho(t) B^\dagger \\
& + \Gamma_{\uparrow\downarrow} \sum_{i=1}^N \left(\sigma_{I,i} \rho(t) \sigma_{I,i}^\dagger + \sigma_{II,i} \rho(t) \sigma_{II,i}^\dagger \right) \\
& + \Gamma_{\downarrow\uparrow} \sum_{i=1}^N \left(\sigma_{I,i}^\dagger \rho(t) \sigma_{I,i} + \sigma_{II,i}^\dagger \rho(t) \sigma_{II,i} \right) \\
& + \Gamma_{\uparrow\uparrow} \sum_{i=1}^N \left(|h\rangle_{I,i} \langle \uparrow | \rho(t) | \uparrow \rangle_{I,i} \langle h| + |h\rangle_{II,i} \langle \uparrow | \rho(t) | \uparrow \rangle_{II,i} \langle h| \right) \\
& + \Gamma_{\uparrow\downarrow} \sum_{i=1}^N \left(| \uparrow \rangle_{I,i} \langle h | \rho(t) | h \rangle_{I,i} \langle \uparrow | + | \uparrow \rangle_{II,i} \langle h | \rho(t) | h \rangle_{II,i} \langle \uparrow | \right) \\
& + \Gamma_{\downarrow\downarrow} \sum_{i=1}^N \left(|h\rangle_{I,i} \langle \downarrow | \rho(t) | \downarrow \rangle_{I,i} \langle h| + |h\rangle_{II,i} \langle \downarrow | \rho(t) | \downarrow \rangle_{II,i} \langle h| \right) \\
& + \Gamma_{\downarrow\uparrow} \sum_{i=1}^N \left(| \downarrow \rangle_{I,i} \langle h | \rho(t) | h \rangle_{I,i} \langle \downarrow | + | \downarrow \rangle_{II,i} \langle h | \rho(t) | h \rangle_{II,i} \langle \downarrow | \right) \\
& + \Gamma_{\uparrow\uparrow} \sum_{i=1}^N \left(| \uparrow \rangle_{I,i} \langle \uparrow | \rho(t) | \uparrow \rangle_{I,i} \langle \uparrow | + | \uparrow \rangle_{II,i} \langle \uparrow | \rho(t) | \uparrow \rangle_{II,i} \langle \uparrow | \right) \\
& + \Gamma_{\downarrow\downarrow} \sum_{i=1}^N \left(| \downarrow \rangle_{I,i} \langle \downarrow | \rho(t) | \downarrow \rangle_{I,i} \langle \downarrow | + | \downarrow \rangle_{II,i} \langle \downarrow | \rho(t) | \downarrow \rangle_{II,i} \langle \downarrow | \right),
\end{aligned} \tag{D1}$$

where Γ_{ab} is the single-particle rate for the transition $|a\rangle \rightarrow |b\rangle$. As in Sec. III B, we omit collective terms due to resonant pump fields, as well as collective dephasing terms (see App. C 2). Collective terms involving the level $|h\rangle$ are also insignificant for $N \gg 1$, as long as the number of coherent collective excitations is small.

In order to compute the amount of entanglement produced, we consider the variance of the nonlocal operator $J_{y,+2} = (J_{y,I} + J_{y,II})_2 / \sqrt{2}$. (The subscript "2" emphasizes that these quantities are defined with respect to the two-level subsystem $\{|\uparrow\rangle, |\downarrow\rangle\}$.) A calculation analogous to the two-level derivation in App. C 1 shows that $\langle J_{y,I} \rangle_2 = \langle J_{y,II} \rangle_2 = 0$ for all times. Therefore $\text{var}(J_y)_2 = \langle J_y^2 \rangle_2$. For simplicity, we assume that both ensembles are identical $\langle J_{y,I}^2 \rangle_2 = \langle J_{y,II}^2 \rangle_2 = \langle J_y^2 \rangle_2$. According to Eq. (D1), the time derivative of the single-ensemble variance $\langle J_y^2 \rangle_2$ is given by

$$\begin{aligned}
d_t \langle J_y^2 \rangle_2 = & - \left(\bar{\Gamma} + d\Gamma \frac{N_2(t)}{N} P_2(t) \right) \langle J_y^2 \rangle_2 + \Gamma \frac{N_2(t)}{4} \\
& + d\Gamma \frac{1}{4} \frac{N_2(t)}{N} P_2(t)^2 (\mu^2 + \nu^2),
\end{aligned}$$

where the decay rate $\bar{\Gamma}$, the number of atoms in the relevant two-level subsystem $\{|\uparrow\rangle, |\downarrow\rangle\}$, $N_2(t)$ and the corresponding polarization $P_2(t)$ are defined in Sec. IV B. $N = \sum_i (|\uparrow\rangle_i \langle \uparrow| + |\downarrow\rangle_i \langle \downarrow| + |h\rangle_i \langle h|)$ is the total number of atoms in one ensemble and $N_2(0) = N$. Note that repump fields, which transfer atoms from $|h\rangle$ to $|\uparrow\rangle$ or

$|\downarrow\rangle$ (corresponding to terms with prefactors Γ_{hg} and Γ_{hs} in Eq. (D1)) do not contribute to $\bar{\Gamma}$.

Inter-ensemble correlations $\langle J_{y,I} J_{y,II} \rangle_2$ evolve according to

$$\begin{aligned}
d_t \langle J_{y,I} J_{y,II} \rangle_2 = & - \left(\bar{\Gamma} + d\Gamma \frac{N_2(t)}{N} P_2(t) \right) \langle J_{y,I} J_{y,II} \rangle_2 \\
& - d\Gamma \frac{1}{2} \frac{N_2(t)}{N} P_2(t)^2 \mu \nu.
\end{aligned}$$

Hence, the time evolution of $\text{var}(J_{y,+})_2 = \langle J_y^2 \rangle_2 + \langle J_{y,I} J_{y,II} \rangle_2$ is given by

$$\begin{aligned}
d_t \langle J_{y,+}^2 \rangle_2 = & - \left(\bar{\Gamma} + d\Gamma \frac{N_2(t)}{N} P_2(t) \right) \langle J_{y,+}^2 \rangle_2 + \bar{\Gamma} \frac{N_2(t)}{4} \\
& + d\Gamma \frac{1}{4} \frac{N_2(t)}{N} P_2(t)^2 (\mu - \nu)^2.
\end{aligned} \tag{D2}$$

Analogously,

$$\begin{aligned}
d_t \langle J_{z,-}^2 \rangle_2 = & - \left(\bar{\Gamma} + d\Gamma \frac{N_2(t)}{N} P_2(t) \right) \langle J_{z,-}^2 \rangle_2 + \bar{\Gamma} \frac{N_2(t)}{4} \\
& + d\Gamma \frac{1}{4} \frac{N_2(t)}{N} P_2(t)^2 (\mu - \nu)^2.
\end{aligned} \tag{D3}$$

Since the evolution of $N_2(t)$ and $P_2(t)$ is known from equations (20), $\Sigma_{J,2} = \langle J_{y,+}^2 \rangle_2 + \langle J_{z,-}^2 \rangle_2$ can be directly calculated yielding a complicated expression. However, as explained in Sec. III and Sec. IV, $N_2(t)$ and $P_2(t)$ can be considered to change slowly compared to the fast entangling dynamics. In this case, (D3) leads to the simple and convenient expression (21) used in Sec. IV B.

Appendix E: Implementation in hot ^{133}Cs vapors

In this appendix, we apply the results derived in Sec. IV to a specific example and consider the generation of entanglement between two ^{133}Cs ensembles at room temperature. The parameters used in the following take values consistent with the experiments reported in [49, 50]. The approximate calculation outlined below provides a rough estimate of the entanglement that can be produced.

We assume \hat{y} -polarized probe light which propagates along \hat{z} and interacts in succession with two ensembles in a magnetic field which is oriented along \hat{x} . The laser field is assumed to be blue detuned by $\Delta = 700\text{MHz}$ with respect to the $6S_{1/2}(F=4) \rightarrow 6P_{3/2}(F=5)$ transition (D2 line). Fig. 5 depicts the relevant parts of the atomic level schemes in both samples and illustrates the atomic transitions due to the light-matter interaction induced by the applied laser field. Initially, all atoms are pumped to state $|\uparrow\rangle$. The restriction of the analysis to the three levels $|\uparrow\rangle$, $|\downarrow\rangle$ and $|h\rangle$ in the presence of strong pump fields, as described in Sec. IV A for \hat{x} -polarized probe light is also valid for this configuration, as the rates of transitions from level $|\uparrow\rangle$ to states with $m_F = \pm 2$

occur at rates which are two orders of magnitude smaller than transitions within the sub-system under consideration. ($\Gamma_{|4,4\rangle\rightarrow|4,2\rangle} = 0.03 \Gamma_{|4,4\rangle\rightarrow|4,3\rangle}$ and $\Gamma_{|4,4\rangle\rightarrow|3,2\rangle} = 0.02 \Gamma_{|4,4\rangle\rightarrow|4,3\rangle}$).

In order to calculate the experimentally measurable steady state entanglement using Eq. (23) for a given optical depth d and parameters μ and ν , $N_2(t)$, $P_2(t)$ and $\bar{\Gamma}$ need to be computed. $N_2(t) = N_\uparrow(t) + N_\downarrow(t)$ and $P_2(t) = (N_\uparrow(t) - N_\downarrow(t))/N_2(t)$ are readily obtained from Eq. (20), if the rates for all transitions are known. As the probe field is assumed to be off-resonant, probe induced rates Γ_{ab} for transitions $|a\rangle \rightarrow |b\rangle$ are calculated using the formula $\Gamma_{ab}^{\text{probe}} = \Omega_{\text{probe}}^2 \sum_l \frac{(c_l^{\text{ab}})^2}{\Delta_l^{\text{ab}}} \gamma_{\text{LW}}$, where the sum runs over all levels contributing to a particular transitions (for example the states $|5,3\rangle$, $|4,3\rangle$ and $|3,3\rangle$ in $6^2P_{3/2}$ if $\Gamma_{\uparrow\downarrow} = \Gamma\nu^2$ is computed). Δ_l^{ab} is the detuning for each contributing level, γ_{LW} the natural line width of excited levels and c_l^{ab} is the product of the corresponding Clebsch Gordan coefficients. Pump, or repump induced transitions are resonant and involve to a good approximation only one level. Hence the corresponding rates are given by $\Gamma_{ab}^{\text{pump}} = \frac{\Omega_{\text{pump}}^2}{\gamma_{\text{LW}}} c_{\text{pump}}^2 k$

and $\Gamma_{ab}^{\text{repump}} = \frac{\Omega_{\text{repump}}^2}{\gamma_{\text{LW}}} c_{\text{repump}}^2 k$ respectively, where $k = \frac{\Gamma}{\delta_{\text{Doppler}}} = \frac{5\text{MHz}}{380\text{MHz}}$ [69]. Here, we consider pumping resonant with respect to the level $|4,4\rangle$ in $6P_{1/2}$ (D_1 line) and pump fields resonant with respect to the level $|4,4\rangle$ in $6P_{3/2}$ (D_2 line). (The decay rates are approximately the same $\gamma_{D_1} \approx \gamma_{D_2} = \gamma_{\text{LW}}$.) Having expressions for $N_2(t)$, $P_2(t)$ as well as $\bar{\Gamma} = \Gamma_{\uparrow\downarrow} + \Gamma_{\uparrow\uparrow} + \Gamma_{\uparrow h} + \Gamma_{\downarrow h} + \Gamma_{\uparrow\uparrow} + \Gamma_{\downarrow\downarrow} + r$ at hand, the amount of entanglement which can be produced in this particular setting can be calculated. Results are shown in Figs. 7 and 8 and are discussed in Sec. IV B. As the three-level description becomes inaccurate if too many atoms are transferred from state $|\uparrow\rangle$ to state $|\downarrow\rangle$, both plots show results for the optimal (that is minimal) pump power which guarantees a fraction of at least 95% of all atoms in the relevant two-level subsystem in state $|\uparrow\rangle$ for all times. Besides the need for sufficient pump fields, repumping of atoms from $F = 3$ to $F = 4$ is required. If strong pump- but no repump fields are applied, no entangled state can be reached, as for $t \rightarrow \infty$, all atoms are transferred to level $|h\rangle$.

-
- [1] H.-J. Briegel, W. Dür, J. I. Cirac, and P. Zoller, Phys. Rev. Lett. **81**, 5932 (1998).
- [2] L.-M. Duan, J. I. Cirac, M. Lukin, P. Zoller, Nature **414**, 413 (2001).
- [3] P. Zoller, *et al.* Eur. Phys. J. D **36**, 203 (2005).
- [4] T. Chanelière, D. N. Matsukevich, S. D. Jenkins, S.-Y. Lan, T. A. B. Kennedy, A. Kuzmich, Nature **438**, 833 (2005).
- [5] C. W. Chou, H. de Riedmatten, D. Felinto, S. V. Polyakov, S. J. van Enk, H. J. Kimble, Nature **438**, 828 (2005).
- [6] M. D. Eisaman, A. André, F. Massou, M. Fleischhauer, A. S. Zibrov and M. D. Lukin, Nature **438**, 837 (2005).
- [7] H. J. Kimble, Nature **453**, 1023 (2008).
- [8] Z. Yuan, Z. *et al.* Nature **454**, 1098 (2008).
- [9] K. S. Choi, H. Deng, J. Laurat and H. J. Kimble, Nature **452**, 67 (2008).
- [10] Y.-A. Chen, S. Chen, Z.-S. Yuan, B. Zhao, C.-S. Chuu, Jörg Schmiedmayer, and J.-W. Pan, Nature Physics **4**, 103 (2008).
- [11] K. Hammerer, A. S. Sørensen, E. S. Polzik, Rev. Mod. Phys. **82**, 1041 (2010).
- [12] J. F. Poyatos, J. I. Cirac and P. Zoller, Phys. Rev. Lett. **77**, 4728 (1996).
- [13] M. B. Plenio, S. F. Huelga, A. Beige, and P. L. Knight, Phys. Rev. A, **59**, 2468 (1999)
- [14] A. Beige, D. Braun, and P. L. Knight, New Journal of Physics **2**, 22 (2000).
- [15] A. Beige, S. Bose, D. Braun, S. F. Huelga, P. L. Knight, M. B. Plenio, and V. Vedral, J. Mod. Opt. **47**, 2583 (2000).
- [16] A. Beige, D. Braun, B. Tregenna, and P. L. Knight, Phys. Rev. Lett. **85**, 1762 (2000).
- [17] Myatt C. *et al.* Nature **403**, 269 (2000).
- [18] M. B. Plenio and S. F. Huelga, Phys. Rev. Lett. **88**, 197901 (2002).
- [19] X. X. Yi, C. S. Yu, L. Zhou, and H. S. Song, PRA, **68**, 052304 (2003).
- [20] B. Kraus and J. I. Cirac, Phys. Rev. Lett. **92**, 013602 (2004).
- [21] S. Mancini and J. Wang, Eur. Phys. J. D **32**, 257 (2004).
- [22] B. Baumgartner, H. Narnhofer, and W. Thirring, J. Phys. A **41**, 065201 (2007).
- [23] R. Doll, M. Wubs, P. Hänggi, and S. Kohler, Phys. Rev. B **76**, 045317 (2007).
- [24] B. Kraus, H. P. Büchler, S. Diehl, A. Kantian, A. Micheli, and P. Zoller, Phys. Rev. A **78**, 042307 (2008).
- [25] Branderhorst, M. *et al.* Science **320**, 638 (2008).
- [26] Syassen, N. *et al.* Science **320** 1329 (2008).
- [27] S. Diehl, A. Micheli, A. Kantian, B. Kraus, H. P. Büchler, P. Zoller, Nature Physics **4**, 878 (2008).
- [28] R. Doll, P. Hänggi, S. Kohler, and M. Wubs, Eur. Phys. J. B **68**, 1434 (2009).
- [29] F. Verstraete, M. M. Wolf, J.I. Cirac, Nature Physics **5**, 633 (2009).
- [30] M. Hor-Meyll, A. Auyuanet, C. Borges, A. Aragão, J. A. Huguenin, A. Khoury, and L. Davidovich, Phys. Rev. A **80**, 042327 (2009).
- [31] G. Vacanti, A. Beige, New J. Phys. **11**, 083008 (2009).
- [32] A. Isar, Open Sys. Inf. Dynamics, **16**, 205 (2009).
- [33] M. Ludwig, K. Hammerer, and F. Marquardt, arXiv:0912.4499 (2009).
- [34] D. G. Angelakis, S. Mancini, S. Bose, Europhys. Lett. **85**, 20007 (2009).
- [35] D. G. Angelakis, L. Dai, L.-C. Kwak, arXiv:0906.2168 (2009).

- [36] H. Weimer, M. Müller, I. Lesanovsky, P. Zoller, and H. P. Büchler, arXiv:0907.1657 (2009).
- [37] F. Benatti, R. Floreanini, and U. Marzolino, arXiv:0912.0354 (2009).
- [38] K. Temme, M. M. Wolf, and F. Verstraete, arXiv:0912.0858 (2009).
- [39] S. Pielawa, L. Davidovich, D. Vitali, and G. Morigi, arXiv:1001.3281 (2010).
- [40] G. Goldstein, P. Cappellaro, J. R. Maze, J. S. Hodges, L. Jiang, A. S. Sørensen, and M. D. Lukin, arXiv: 1001.0089 (2010).
- [41] X. Wang and S. G. Schirmer, arXiv:1005.2114 (2010).
- [42] E. de Valle, arXiv:1005.4383 (2010).
- [43] M. Kiffner and M. J. Hartmann, arXiv:1005.4865 (2010).
- [44] M. Kiffner and M. J. Hartmann, Phys. Rev. A **81**, 021806(R) (2010).
- [45] S. Pielawa, L. Davidovich, D. Vitali, and G. Morigi, Rev. A **81**, 043802 (2010).
- [46] J. Barreiro *et al.* arXiv:1005.1965 (2010).
- [47] A. S. Parkins, E. Solano, and J. I. Cirac, Phys. Rev. Lett. **96**, 053602 (2006).
- [48] L. M. Duan, J. I. Cirac, P. Zoller and E. S. Polzik, Phys. Rev. Lett. **85**, 5643 (2000).
- [49] B. Julsgaard, A. Kozhekin, E.S. Polzik, Nature **413**, 400 (2001).
- [50] W. Wasilewski, T. Fernholz, K. Jensen, L. S. Madsen, H. Krauter, C. Muschik, and E. S. Polzik, Optics Express, **16**, (2009).
- [51] We use operators \tilde{A} , \tilde{B} labelled with a tilde for bosonic modes. Later in the text, operators A , B without a tilde are used to denote linear combinations of spins.
- [52] M. G. Raymer, A. C. Funk, B. C. Sanders, and H. de Guise, Phys. Rev. A **67**, 052104 (2003).
- [53] The quantization axis is defined by the direction of the magnetic field, which is oriented along \hat{x} , hence $j_x = \frac{1}{2}(|\uparrow\rangle\langle\uparrow| - |\downarrow\rangle\langle\downarrow|)$.
- [54] For large, strongly polarized atomic ensembles, collective spins can be described by bosonic modes $J_I^- \propto a$, $J_{II}^- \propto b$ using the Holstein-Primakoff approximation. The results derived here are based on related approximations and are valid for $N \gg 1$ (compare App. C).
- [55] The basic working principle of this approach can be illustrated by considering two single atoms with ground state $|g\rangle$ and excited state $|e\rangle$, which are placed in two different cavities. Both atoms are initially prepared in the excited state $|\Psi^{\text{in}}\rangle = |e\rangle_1|e\rangle_2$. Atoms can spontaneously decay to their ground state $|e\rangle \rightarrow |g\rangle$ while emitting a photon. The light emitted from both cavities is combined at a beam-splitter and photon detectors are placed at each output port. The atoms are projected into a maximally entangled state $|\Psi^{\text{out}}\rangle = (|e\rangle_1|g\rangle_2 + |g\rangle_1|e\rangle_2)/\sqrt{2}$ if a photon is detected at one of the two output ports.
- [56] H. Krauter, C. A. Muschik, K. Jensen, W. Wasilewski, J. M. Petersen, J. I. Cirac, and E. S. Polzik, arXiv:1006.4344 (2010).
- [57] μ and ν are normalized such that $\mu^2 - \nu^2 = 1$ and accordingly, $[A, A^\dagger] = [B, B^\dagger] = 1$.
- [58] A $\lambda/2$ plate interchanges the fields in \hat{x} and \hat{y} polarization. If such a passive optical element is placed between the first and the second atomic ensemble, the roles of classical and quantum fields are interchanged. Therefore, the classical field drives π -transitions $|\uparrow\rangle \rightarrow |e_\uparrow\rangle$, $|\downarrow\rangle \rightarrow |e_\downarrow\rangle$, in the second ensemble, while the quantum field is associated with transitions which change the magnetic quantum number $\Delta_m = \pm 1$.
- [59] Undesired radiative transitions $|\uparrow\rangle \rightarrow |\uparrow\rangle$ and $|\downarrow\rangle \rightarrow |\downarrow\rangle$ involve the emission of a photon but no change of the internal atomic state. These processes are not explicitly shown in Fig. 2.
- [60] C. Cohen-Tannoudji, J. Dupont-Roc, G. Grynberg. Atom-Photon Interactions. Wiley, New York (1998).
- [61] If the upper and lower sideband are not treated as independent baths, cross terms appear, which rotate fast (with frequency $\pm 2\Omega$) compared to the single-bath terms, (which do not rotate in this picture). These cross terms can be neglected in a rotating wave approximation if $\Omega \gg \Gamma_{\text{atomic}}$.
- [62] R.H. Lehmberg, Phys. Rev. A **2**, 883 (1970).
- [63] D. Porras and J. I. Cirac, arXiv:0704.0641 (2007).
- [64] D. Porras and J. I. Cirac, Phys. Rev. A **78**, 053816 (2008).
- [65] L.-M. Duan, J.I. Cirac and P. Zoller, Phys. Rev. A **66**, 023818 (2002).
- [66] An analysis of the generation of entanglement between two atomic ensembles in the opposite limit of fixed atomic positions can be found in: O. Mishina, D. Kupriyanov, E. S. Polzik, Proceedings of the NATO Advanced Research Workshop, Crete 2005: "Quantum Communication and Security" (ISO Press, Amsterdam) **199**, 346 (2006).
- [67] In the two-level model shown in Fig. 2, $\Gamma_{\text{d}}^{\text{rad,probe}} = 2 \left(\Gamma_{\text{cool}}^{\text{probe}} + \Gamma_{\text{heat}}^{\text{probe}} \right)$, due to the ratio of Clebsch Gordan coefficients $c_{\Delta_m=\pm 1}^2/c_{\Delta_m=0}^2 = 2$.
- [68] Rates Γ_{ab} are calculated using the formula $\Gamma_{ab} = \Omega_{ab}^2 \frac{c_{ab}^2}{|\Delta_{ab} + i\gamma_{\text{LW}}|^2} \gamma_{\text{LW}}$, where Ω_{ab} is the Rabi frequency, Δ_{ab} the detuning, γ_{LW} the natural line width of excited levels and c_{ab} the Clebsch Gordan coefficient for the transition under consideration. The cooling rate $\Gamma_{\text{cool}} = \Gamma_{\text{cool}}^{\text{probe}} + \Gamma_{\text{cool}}^{\text{pump}}$ consists of a probe- and a pump induced part. As probe fields are considered to be far off-resonant, the corresponding cooling rate is calculated using the approximation $\Gamma_{\text{cool}}^{\text{probe}} = \Omega_{\text{probe}}^2 \frac{1}{(\Delta - \Omega)^2} \gamma_{\text{LW}}$. Contributions due to resonant pump fields are given by $\Gamma_{\text{cool}}^{\text{pump}} = \Omega_{\text{pump}}^2 \frac{1}{\gamma_{\text{LW}}^2} \gamma_{\text{LW}}$.
- [69] The correction factor k takes into account that due to the Doppler broadening of atoms moving at room temperature only a fraction $k = \frac{\gamma_{\text{LW}}}{\delta_{\text{Doppler}}}$ of all atoms in the cell is on resonance with the applied field. The Doppler width is given by $\delta_{\text{Doppler}} = \frac{\nu}{c} \left(\frac{2k_B T}{m \ln 2} \right)^{1/2}$, where $c/\nu = \lambda$ is the wavelength of the applied light field, k_B is the Boltzmann constant, T is the temperature and m is the atomic mass.
- [70] Eq. (A1) yields $d_t \langle a^\dagger a \rangle = -\kappa_A \langle a^\dagger a \rangle$ and $d_t \langle b^\dagger b \rangle = -\kappa_B \langle b^\dagger b \rangle$. Hence, $\langle a^\dagger a \rangle_\infty = \langle b^\dagger b \rangle_\infty = 0$ in the steady state.
- [71] L.-M. Duan, G. Giedke, J. I. Cirac and P. Zoller, Phys. Rev. Lett. **84**, 2722 (2000).
- [72] R. Simon, Phys. Rev. Lett. **84**, 2726 (2000).
- [73] T. Holstein, H. Primakoff, Phys. Rev. **58**, 1098 (1940).
- [74] The dipole term $(\hat{\mathbf{p}} \cdot \hat{\mathbf{r}}_{ij})^2$ leads to contributions which decay quickly in the interatomic distance. The corresponding terms in Eq. (B7) (the second and third term in brackets) are also negligible in the calculation of the single-ensemble rate $\Gamma_{ij,A}$ as discussed in App. B 2.
- [75] For perfectly polarized ensembles $\langle J_z J_x \rangle = \langle J_z \rangle \langle J_x \rangle$. The decorrelation approximation is justified as long as only a

small number of collective (coherent) excitations is created in the atomic sample. In practise, the degree of squeezing, which can be produced in atomic samples is small, such that the decorrelation approximation is a reasonable assumption for the settings considered in this article.

- [76] Initially, $\langle J_x^2 \rangle|_{t=0} = \langle J_x \rangle^2|_{t=0}$. The time evolution of $\langle J_x^2 \rangle$ is given by $d_t \langle J_x^2 \rangle = -2(\Gamma_{\text{cool}} + \Gamma_{\text{heat}}) \langle J_x^2 \rangle + \frac{N}{2}(\Gamma_{\text{cool}} + \Gamma_{\text{heat}}) + N(\Gamma_{\text{cool}} - \Gamma_{\text{heat}}) \langle J_x \rangle$. Hence, $\langle J_x^2 \rangle_\infty - \langle J_x \rangle_\infty^2 = \frac{N}{4} + \langle J_x \rangle_\infty$ (compare Eq. (15)) in the steady state and the error is by a factor N smaller than $\langle J_x^2 \rangle$ for all times.
- [77] M. Fleischhauer and M. D. Lukin, Phys. Rev. Lett. **84**, 5094, (2000).
- [78] M. D. Lukin, rev. Mod. Phys. **75**, 457 (2003).
- [79] A. V. Gorshkov, A. André, M. D. Lukin, and A. S. Sørensen, Phys. Rev. A **76**, 033804 (2007).
- [80] J. B. Brask, L. Jiang, A. V. Gorshkov, V. Vuletic, A. S. Sørensen, and M. D. Lukin, arXiv:0907.3839 (2009).
- [81] T. J. Kippenberg and K. Vahala, Science
- [82] F. Marquart and S. M. Girvin, Physics
- [83] M. Aspelmeyer, S. Gröblacher, K. Hammerer, and N. Kiesel, J. Opt. Soc. Am. B **27**, A189-A197 (2010) - JOSA B Feature Issue on Quantum Optical Information Technologies, P. Grangier, A. Jordan, G. Morigi (Eds.).
- [84] I. Wilson-Rae, n. Nooshi, W. Zwerger, and T. J. Kippenberg, Phys. Rev. Lett. **99**, 093901 (2007).
- [85] F. Marquart, J. P. Chen, A. A. Clerk, and S. M. Girvin, Phys. Rev. Lett. **99**, 093902 (2007).
- [86] C. Genes, D. Vitali, P. Tombesi, S. Gigan, and M. Aspelmeyer, Phys. Rev. A **77**, 033804(2008).